

**CHAPTER 3: *CIS-TRANS* ISOMERIZATION AT A
CONSERVED PROLINE DURING GATING OF A CYS-
LOOP RECEPTOR**

3.1 Introduction

3.1.1 Ligand-gated ion channels

As discussed in Chapter 1, synaptic transmission is initiated when the presynaptic axon terminal releases neurotransmitters into the synaptic cleft. The neurotransmitters diffuse across the synaptic cleft and bind to receptors embedded in the membrane of a postsynaptic dendrite of a neighboring neuron. Binding of the neurotransmitter activates the receptor, eliciting cellular events in the postsynaptic neuron, thus modulating its activity. There are a variety of neurotransmitters and neuroreceptors. There are two main categories of neuroreceptors—1) metabotropic and 2) ionotropic receptors. Metabotropic receptors are responsible for slow synaptic transmission and act through second messenger pathways. Binding of neurotransmitter initiates cascades that can result in gating of ion channels or other cellular effects. Metabotropic receptors include the G-protein coupled receptor family.

Ionotropic receptors are also known as ligand-gated ion channels (LGICs) and are responsible for fast synaptic transmission. Binding of the neurotransmitter to a LGIC causes a conformational change of the entire channel, resulting in gating of the channel and the flow of ions. LGICs are highly selective, allowing for the transport of specific ions. This selectivity allows for the modulation of action potentials in a postsynaptic neuron. Whether or not a postsynaptic neuron fires an action potential is determined by whether or not the activated LGIC is excitatory (cation selective) or inhibitory (anion selective). The balance of excitatory and inhibitory activity through the activation of LGICs influences information processing in our brain. Not surprisingly, aberrations of this balance can result in disease states and/or abnormal activity including anxiety, epilepsy and neuronal death.¹⁻¹⁵ Furthermore, LGICs are therapeutic targets for numerous maladies including Alzheimer's

disease, Parkinson's disease, learning and attention disorders, and depression and drug addiction.¹⁶

The class of LGICs is comprised of four superfamilies: the glutamate receptors, the transient receptor potential (TRP) channels, the ATP-gated channels, and the Cys-loop receptor superfamily. The glutamate receptors include the N-methyl-D-aspartate (NMDA) receptors, the α -amino-3-hydroxy-5-methyl-4-isoxalepropionic acid (AMPA) receptors and kainite receptors. The Cys-loop receptor superfamily consists of both cationic and anionic ligand-gated ion channels.

3.1.2 Cys-loop receptors

As mentioned before, the Cys-loop receptor superfamily can be divided further into two classes based on their ion permeation properties. The cationic selective class of Cys-loop receptors includes the nicotinic acetylcholine receptors (nAChR) and the serotonin gated 5-hydroxytryptamine-3 (5-HT₃) receptors.¹⁷⁻²² The anion selective class of receptors includes the γ -aminobutyric acid (GABA) receptors and the glycine receptors.^{23, 24} Cys-loop receptors perform important physiological functions, and mutations in these channels can result in a myriad of pathological states, or channelopathies, such as epilepsy, hyperekplexia, and Angelman's syndrome. Cys-loop receptors are also therapeutic targets for Alzheimer's disease,²⁵ Parkinson's disease,²⁶ anxiety, learning and attention disorders,^{27, 28} as well as targets of analgesics, anti-emetics, and anesthesia.^{16, 29-37}

Members of the Cys-loop superfamily are thought to share similar architecture. Each receptor is comprised of a pentameric structure with five subunits assembled to construct a ring structure forming the pore.^{38, 39} Some subunits can form a homogeneous receptor, while

other receptors are formed by a heterogeneous composition of receptor subunits.⁴⁰⁻⁴³ Each subunit consists of four transmembrane domains (M1-M4), a large extracellular N-terminal domain and an extracellular C-terminal domain (Figure 3.1A).⁴⁴⁻⁴⁷ The large N-terminal domain contains the ligand binding site as well as a characteristic Cys-loop, for which the family is named, formed by a cysteine disulfide bond. The sequence alignment of known Cys-loop subunits shows a fair amount of homology, with roughly 25% to 30% identity. Each subunit is arranged in a pentameric array with the M2 region of each subunit lining the pore (figure 1B). It should be noted that for each receptor in the family, there exists a variety of subunit isoforms that combine in different compositions to form distinct receptor subtypes.^{48, 49} For many of these receptors, the exact composition of subunit isoforms is unknown.

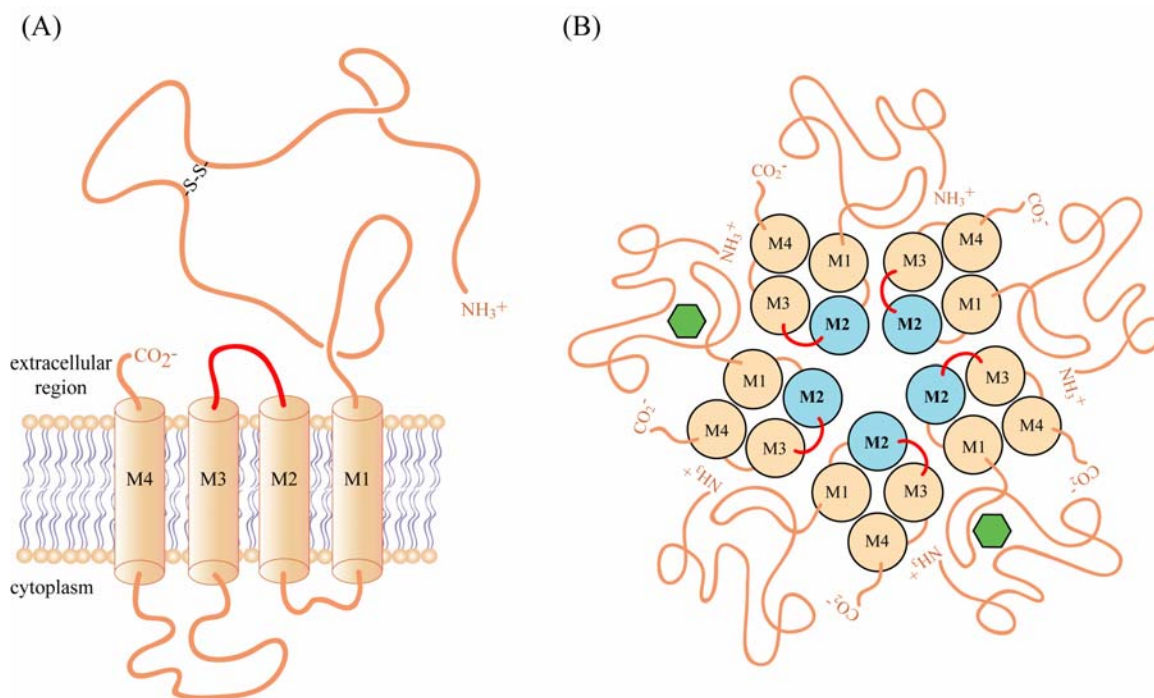


Figure 3.1. A) Schematic for one subunit of a Cys-loop receptor. B) Subunits arrange to form a pentameric array with a central pore lined by the M2 helices.

3.1.3 Gating model for Cys-loop receptors

Given the role of Cys-loop receptors in a variety of neurological processes and as therapeutic targets for numerous pathologies, it is of great interest to gain a greater functional understanding of these channels. Specifically, it is of interest to elucidate the mechanism by which binding of an agonist initiates a series of conformational changes that ultimately results in the opening of an ion channel. The agonist binding site and channel gate are separated by 50 Å and 100 amino acids of the protein's primary sequence; the process of gating represents an elegant feat achieved by a sequence of steric and noncovalent interactions. The amazing nature of this process is further appreciated when one considers the size of an ion channel relative to typical organic molecules. Despite advances in both experimental and theoretical methods, the molecular details of the mechanism of ion channel gating are still poorly understood.

As integral membrane proteins, ion channels have been resistant to crystallographic analysis and as such, there are limited structural data for Cys-loop receptors. The lack of structural data has made it difficult to attribute functional changes in structure-function studies to specific structural changes during gating. In 2001, the crystal structure of the acetylcholine binding protein (AChBP) was obtained. AChBP is a small soluble protein that is homologous to the extracellular N-terminal domain of the nicotinic acetylcholine receptor. Since the discovery of the crystal structure of AChBP, several members of the Cys-loop family have been modeled onto the crystal structure to predict their quaternary structures. The resulting models were consistent with 40 years of biochemical studies that accurately predicted the formation of the ligand-binding domains at the interfaces between subunits.

In 1995, Unwin provided the first evidence of a dynamic structure for a Cys-loop receptor.⁵⁰ Using freeze trapping methods and cryo-electron microscopy, 9 Å resolution images were obtained for the nicotinic acetylcholine receptor. The freeze trapping method allowed for images to be created for the open and closed states of the nAChR. From these cryo-electron microscopic data, Unwin proposed a gating model for nAChR and therefore, by extension all ligand-gated ion channels (figure 3.2). In 2003, cryo-electron microscopic images were extended to a resolution of 4 Å.^{51,52}

In Unwin's proposed model, binding of a ligand results in a 15 degree rotation of the α subunits. The rotation of these subunits causes movement of valine 44 of the α -subunit, which resides at the apex of the extracellular β 1- β 2 loop (loop 2). Valine 44 of the α -subunit makes contact with the M2-M3 loop through a hydrophobic interaction. The model proposes that α -valine 44 docks into a hydrophobic pocket formed by residues serine 269 to proline 272. Movement of α -valine 44, causes movement of the M2-M3 loop resulting in rotation of the M2 helix. This movement destabilizes the hydrophobic "girdle" that forms the gate, thus resulting in a widening of the pore that permits ions to pass.

3.1.4 M2-M3 loop movement in the mechanism of channel gating

In Unwin's "pin-and-socket" model, the M2-M3 loop is proposed to play a major role in channel gating by acting as a direct physical link that enables the propagation of a conformational change at the binding site to the channel gate (figure 3.2). Rotation of the inner sheets of the α -subunit is translated to a rotation of the M2 helix via the M2-M3 loop with the M2-M3 loop acting as a pivot point. Biochemical studies also support a prominent role for the M2-M3 loop in channel gating.⁵³⁻⁶⁵ Substituted cysteine accessibility studies

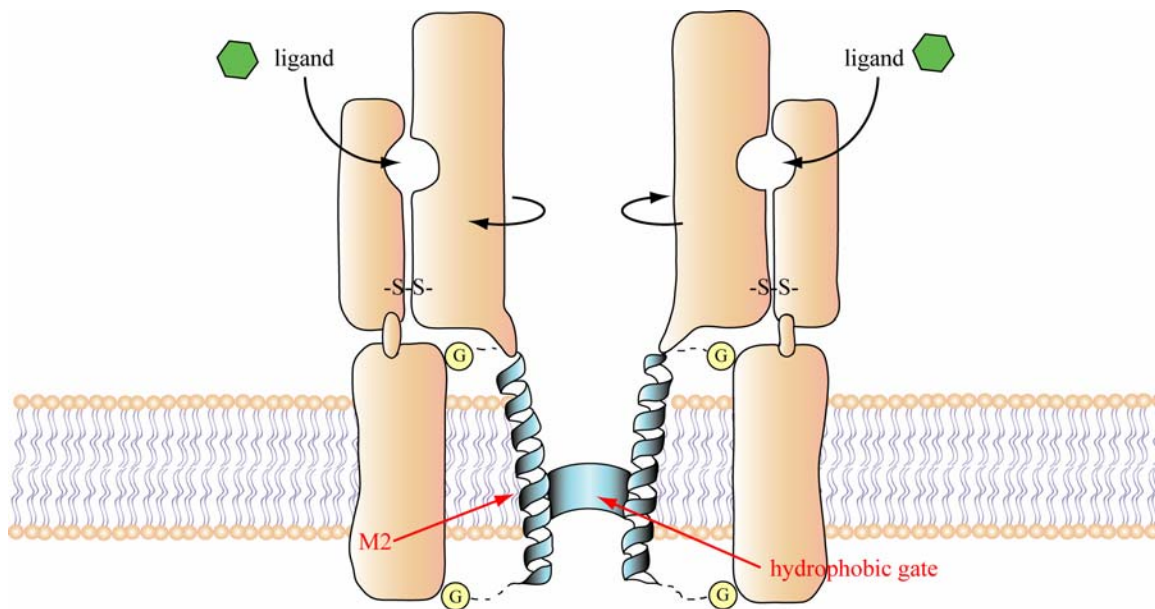


Figure 3.2. Unwin's pin-and-socket mechanism of gating for LGICs.

have suggested that the surface accessibility of the M2-M3 loop increases upon gating in the glycine receptor, implying movement of the M2-M3 loop during gating.⁶⁶ Similar studies in the GABA_A receptor yielded similar conclusions.⁶⁴ Furthermore, mutational analysis of the glycine receptor and the nAChR supports a model where the M2-M3 loop acts as a coupling between the binding site and the channel gate. Mutations of critical residues in the M2-M3 loop resulted in the decoupling of ligand binding and channel gating.

Additional mutational analysis of the M2-M3 region, using single channel analysis, indicated that the M2-M3 loop in nAChR serves as a linker whose hydrophobicity influences channel gating.⁶⁷ Substitution of residues near the middle of the loop in the α -subunit with hydrophobic residues appeared to enhance channel gating whereas hydrophilic mutations showed no apparent effect. Another important result of these studies was that mutations in this region had little effect on the agonist affinity for the opened and closed state but had an

effect on the gating equilibrium. Recently, similar mutational studies done in the M2-M3 loop of a chimeric $\alpha 7$ -5-HT_{3A} receptor further supported a functional role for the M2-M3 loop as a control element in gating.⁶⁸ Mutational analysis of the chimeric receptor also yielded receptors with altered channel gating without altered agonist binding affinity.

A growing body of evidence suggests a prominent role for the M2-M3 loop during channel gating and recently, biophysical studies have provided evidence for a direct interaction between the M2-M3 loop and the Cys-loop. Kash *et al.* performed mutational analysis in the GABA_A receptor in which two charged residues, one located in the M2-M3 loop and the other in the Cys-loop were reversed.⁶⁵ They were able to demonstrate the presence of an electrostatic interaction between a lysine in the M2-M3 loop and an asparagine residue in the Cys-loop. It should be noted that this lysine is not conserved in the nAChR and in the 5-HT_{3A} receptor nor did analogous studies in the glycine receptor yield similar results. However, it is possible that variations exist among receptors in how the M2-M3 loop interacts with the Cys-loop. Furthermore, Unwin's cryo-electron microscopic images and biochemical studies also suggest an interaction of M2-M3 loop with the Cys-loop and the extracellular $\beta 1$ - $\beta 2$ loop (loop 2). Therefore, it is likely that the interactions with *both* the Cys-loop and $\beta 1$ - $\beta 2$ loop are important for the coupling of ligand binding to channel gating. Nonetheless, despite the ambiguity for the exact nature of the M2-M3 loop's role in channel gating, results of these studies all support a prominent functional role for it in the gating mechanism.

proline in biological processes, the conserved prolines may play key roles in the function of M2-M3 loop during channel gating.

3.1.6 Proline in biological processes

Of the twenty natural amino acids, proline is unique in that it lacks a primary amine due to the covalent bonding of the three carbon side chain to the nitrogen atom of the peptide backbone. Therefore proline has no amide hydrogen to act as a hydrogen bond donor. Furthermore, the distinctive five-membered ring, formed by the side-chain forming a covalent bond with the backbone, imparts a greater rigidity on the backbone and restricts the backbone conformation of neighboring amino acids.^{69, 70} As a result, proline is considered the classic helix breaker and is used by nature in a variety of irregular structures.⁷⁰⁻⁷²

Proline is also unique in that it is the only natural amino acid in which the *cis* conformation is readily accessible (figure 3.4). All other peptide bonds occur predominantly in the *trans* conformation due to an energy barrier of approximately 20 kcal/mol between the *trans* and *cis* conformation. This results in a scarcity of *cis* peptide bonds occurring in proteins.⁷³ However, in the case of the Xaa-Pro peptide bond (where Xaa is any amino acid), the difference in energy between the conformers is only about 0.5 kcal/mol. Thus a survey of the protein data base reveals a significant proportion (about 5-6%) of the Xaa-Pro peptide

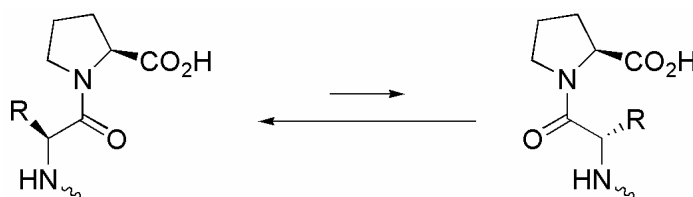


Figure 3.4. Proline is a unique amino acid in that the *cis*-conformation is readily accessible.

bonds adopting the *cis* conformation compared to only 0.03-0.05 percent of Xaa-nonPro peptide bonds occurring in the *cis* conformation.⁷⁴⁻⁷⁷

The ability of proline to adopt the *cis* conformation distinguishes it from the other natural amino acids. Proline *cis-trans* isomerization has been implicated in the regulation of biological activity in proteins/peptides containing this amino acid, by acting as a molecular switch.⁷⁸ Evidence suggests it also plays a role in protein folding and stability.⁷⁹⁻⁸⁵ Interestingly, evidence suggests that local structural changes caused by *cis-trans* isomerization are minimal; however there is amplification of these small structural changes through the peptide backbone, allowing for structural changes in areas removed from the immediate proline locale.⁸⁶

A variety of studies highlight the importance of the proline conformation in biological recognition. For example, biochemical assays and structural studies suggested that a *cis* conformation around a tyrosine-proline amide bond is necessary for the biological activity of morphiceptin, a tetrapeptide.⁸⁷⁻⁸⁹ A *cis* conformation was found to be necessary for the μ -receptor binding and selectivity of morphiceptin. Furthermore, a *cis* conformation has also been shown to be required for the activity of the muscle selective μ -conotoxins GIIIB, which act a blocker of voltage-sensitive sodium channels.⁹⁰ A *cis* conformation is also necessary for the interaction of interleukin-3 with its receptor.⁹¹

Proline *cis-trans* isomerization may also play a role in regulating the agonist/antagonist activity of peptides. Studies by Halab *et al.*, suggests that oxytoxin with a *cis* proline acts as an antagonist to its receptor while a *trans*-conformation is critical for agonist activity.^{92, 93} Evidence also implicates proline *cis-trans* isomerization in T-cell signaling through conformer-specific recognition of the ligand.⁹⁴

3.2 Experimental design

The research described herein is a continuation of work spearheaded by Dr. Darren L. Beene and done in collaboration with Dr. Sarah C.R. Lummis (Cambridge). It was aimed at studying the role of two conserved prolines in the M2-M3 loop region of the cation selective Cys-loop receptor—the serotonin gated 5-hydroxytryptamine_{3A} receptor (5-HT_{3A}) and the nicotinic acetylcholine receptor (nAChR). The *cis-trans* isomerization of proline has been suggested to play a role in biological processes. As such, this research was aimed at studying the role of the *cis-trans* isomerization in the gating of Cys-loop receptors. Using *in vivo* nonsense suppression methodology in *Xenopus* oocytes, a series of proline analogues of

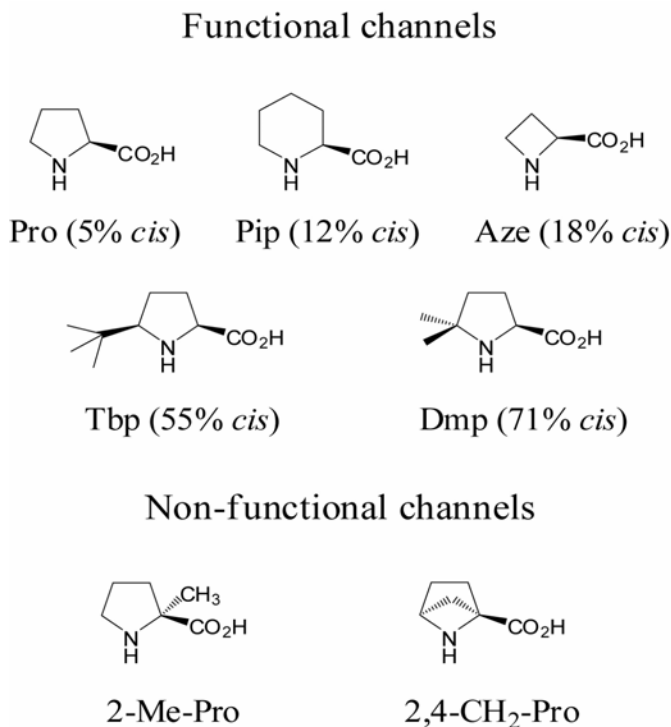


Figure 3.5. Structures of proline analogues that were incorporated into cation selective Cys-loop receptors using nonsense suppression methodology. Proline analogues with a greater *cis* preference than native proline produced functional channels. Percentage *cis* preference is shown in parentheses.

varying *cis* preference were incorporated at the 1* (301) and 8* (308) proline site in the M2-M3 loop of the 5-HT_{3A} receptor (Figure 3.5). The mutant channels were then functionally evaluated using two-electrode voltage clamp electrophysiology. If the *cis-trans* isomerization of either proline plays a role in the gating mechanism of the channel, then we anticipate changes in the gating of the channel with the replacement of the native proline with the synthesized proline analogues. This chapter also describes initial work examining the role of *cis-trans* isomerization at the analogous prolines (265 and 272) in nAChR.

3.3 Results

3.3.1 Introduction

We aimed to examine the role of *cis-trans* isomerization of two conserved proline residues, at site 301 and 308 in the gating of the 5-HT_{3A} receptor. A series of proline analogs were incorporated at these sites to examine the role of these prolines in receptor function. Previous studies done by Dr. Darren L. Beene and Dr. Sarah C. R. Lummis showed that site 301 tolerated a variety of mutations without loss of receptor function. Experimental data strongly suggest that proline 301 is not critical for receptor function in 5-HT_{3A}. Experimental data strongly suggested a critical role for proline 308 in receptor function. Substitution of proline 308 with glycine, alanine, cysteine, valine, lysine or asparagine resulted in receptors that were non-functional but were properly trafficked to the membrane and displayed wild type binding properties for a radiolabeled agonist. This indicated that these mutations affected the gating of the receptor and not ligand binding or assembly of the receptor. These data strongly suggested that an intrinsic characteristic of proline was required for the proper gating of this receptor.

A series of unnatural proline analogs were substituted at site 308 using nonsense suppression in *Xenopus* oocytes, and experimental results suggest it was neither the cyclic nature of proline nor the lack of hydrogen bonding ability that was critical for proper receptor function. However, substitution with 2,4-CH₂-Pro and 2-Me-Pro, which show a reduced *cis* preference relative to proline, produced non-functional receptors although these receptors did reach the cell surface. Furthermore, incorporation of azetidine, pipercolic acid, and 5,5-dimethylproline which have varying *cis* preferences appeared to support a model of gating in which proline 308 serves as a hinge during gating. The research described herein is a continuation of the work done by Dr. Darren L. Beene and Dr. Sarah C. R. Lummis and involves the incorporation of *cis*-5-*tert*-butyl-L-proline, which has a *cis* preference that is between that of Aze and Dmp. As a result a crucial data point that was intermediate between those for pipercolic acid and 5,5-dimethylproline was obtained for a plot of the *cis-trans* energy gap versus receptor activation. *Cis*-5-*tert*-butylproline is not commercially available and as such, the continuation of these studies began with the chemical synthesis of *cis*-5-*tert*-butyl-L-proline.

3.3.2 Synthesis of *cis*-5-*tert*-butyl-L-proline

The synthesis of *cis*-5-*tert*-butyl-L-proline was achieved using previous reported methods with minor modifications (figure 3.6).⁹⁵ Glutamic acid gamma-methyl ester **1** was amino-protected with a phenylfluorenyl protecting group using triethylamine and 9-bromo-9-phenylfluorene.⁹⁶ Acylation of the phenylfluorenyl protected glutamic acid gamma-methylester **2** was performed by first generating the enolate using lithium bis(trimethylsilyl)amide (LiHMDS) in tetrahydrofuran. The enolate was subsequently

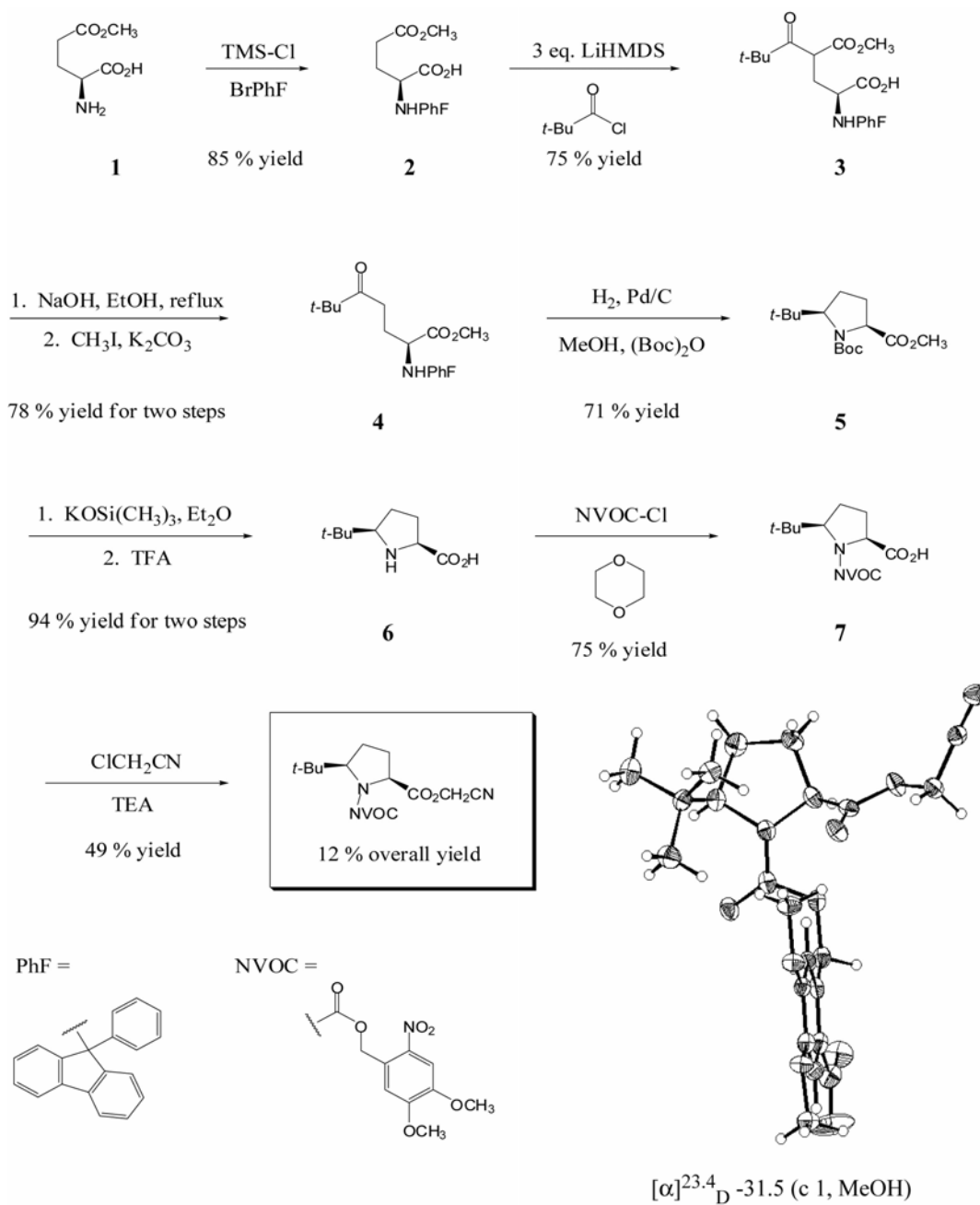


Figure 3.6. Synthesis of *cis*-5-*tert*-butyl-L-proline.

treated with pivaloyl chloride to yield the beta-keto ester **3** as a mixture of diastereomers. Hydrolysis and decarboxylation using sodium hydroxide followed by esterification cleanly converted **3** to the heptanoate **4** in a 78% yield for both steps. Treatment of heptanoate **4**

with 10% palladium on carbon in the presence of hydrogen gas results in a three step—one pot reaction. This proceeds by cleavage of the phenylfluorenyl group, cyclization via reductive amination, followed by BOC protection and hydrogen addition to yield the BOC protected *cis*-5-*tert*-butyl-L-proline methyl ester in 71% yield. At this stage the relative stereochemistry was confirmed to be *cis* using polarimetry. Saponification of methyl ester **5** was achieved using potassium trimethylsilanolate in diethyl ether. Removal of the BOC protecting group with trifluoroacetic acid in dichloromethane yielded the free amino acid which was then NVOC-protected and converted to the cyanomethyl ester in preparation for dCA coupling for tRNA ligation. Prior to coupling to dCA, X-ray crystallography and polarimetry were used to establish the stereochemistry of the *tert*-butyl moiety as *cis* relative to the carboxylic acid functionality.

3.3.3 Incorporation of cis-5-tert-butyl-L-proline into Pro 8 of the M2-M3 loop of 5-HT_{3A} receptor using nonsense suppression*

Cis-5-*tert*-butyl-L-proline was incorporated into the 5-HT_{3A} receptor using nonsense suppression methodology. First, *cis*-5-*tert*-butyl-L-proline was chemically coupled to dCA and then enzymatically ligated to tRNA in preparation for use for nonsense suppression. Prior to use, the NVOC-protecting group was photolyzed using an arc lamp. mRNA was translated from DNA encoding for 5-HT_{3A} subunit with the TAG mutation inserted at position 308 (corresponding to the 8* proline in the M2-M3 loop). Subsequently, the charged tRNA bearing *cis*-5-*tert*-butyl-L-proline was co-injected with the corresponding mRNA into *Xenopus* oocytes. The oocytes were then incubated to allow for the processing, assembly and surface transport of the expressed mutant channel.

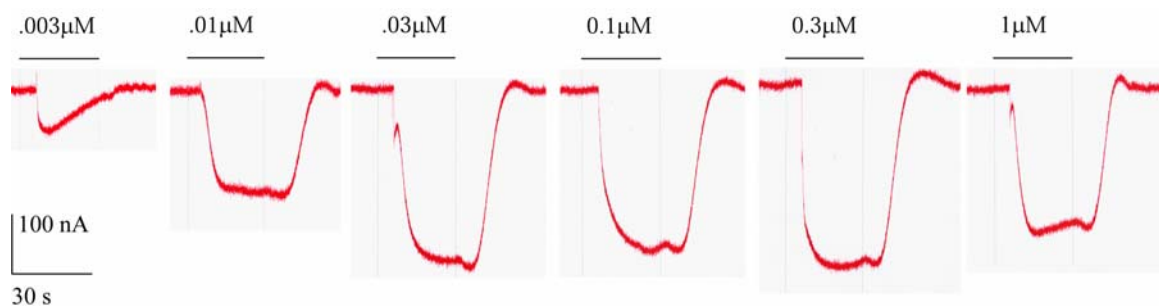


Figure 3.7. Representative traces for mutant 5-HT_{3A} receptors containing Tbp at site 308 (8*). Bars represent application of 5-HT.

3.3.4 Electrophysiological analysis using two voltage clamp electrophysiology

Xenopus oocytes expressing 5-HT_{3A} receptor with *cis*-5-*tert*-butyl-L-proline (Tbp) at site 308 were evaluated using two-electrode voltage clamp electrophysiology. Oocytes were perfused with varying concentrations of serotonin (5-HT) to generate dose-response curves. It should be noted that expression of Tbp mutant receptors was poor relative to that of the wild type recovery receptors in which Pro was inserted using the same nonsense suppression

Residue	Per cent <i>cis</i> *	EC ₅₀ (μM)†	ΔΔ <i>G</i> (<i>c-t</i>) (kcal/mol)‡	ΔΔ <i>G</i> (<i>c-t</i>) (kcal/EC ₅₀)§
Pro	5	1.29 ± 0.07	0	0
Pip	12	0.75 ± 0.06	-0.54	-0.32
Aze	18	0.42 ± 0.03	-0.85	-0.66
Tbp	55	0.030 ± 0.024	-1.86	-1.73
Dmp	71	0.021 ± 0.009	-2.28	-2.47

*Determined from studies of model peptide systems reported previously. Because variations are seen depending on methodology and exact model system, all values are referenced to the *cis-trans* ratio seen for Pro in the same study, and Pro is set to 5%, the value obtained from statistical surveys of protein structures.

†Values are in ±s.e.m.

‡Values are relative to proline.

§ Equals $-RT\ln(EC_{50}(\text{mutant})/EC_{50}(\text{Pro}))$.

Table 3.1 Influence of proline isomerism on receptor function.

methodology. Expression levels seen for Tbp were roughly 5-10% of that seen for the Pro insertion by the same technique. Diminished expression levels of mutant receptor were previously seen for the other proline analogs (Pip, Aze, and Dmp). For

Tbp traces, the waveforms seen were similar to that seen for the wild type receptor (figure 3.7). The EC_{50} value for 5-HT_{3A} receptor containing Tbp at site 308 was determined to be $0.030 \mu\text{M} \pm 0.024$, a 40-fold decrease in EC_{50} value compared to the wild type receptor. Table 3.1 shows a summary of EC_{50} values for proline analogs of varying *cis* preference as well as percent *cis* for each analog. The relationship between the *cis-trans* energy gap and that of receptor activation is shown in Figure 3.8. A linear relationship is observed between the the *cis-trans* energy gap and that of receptor activation with a slope of nearly one.

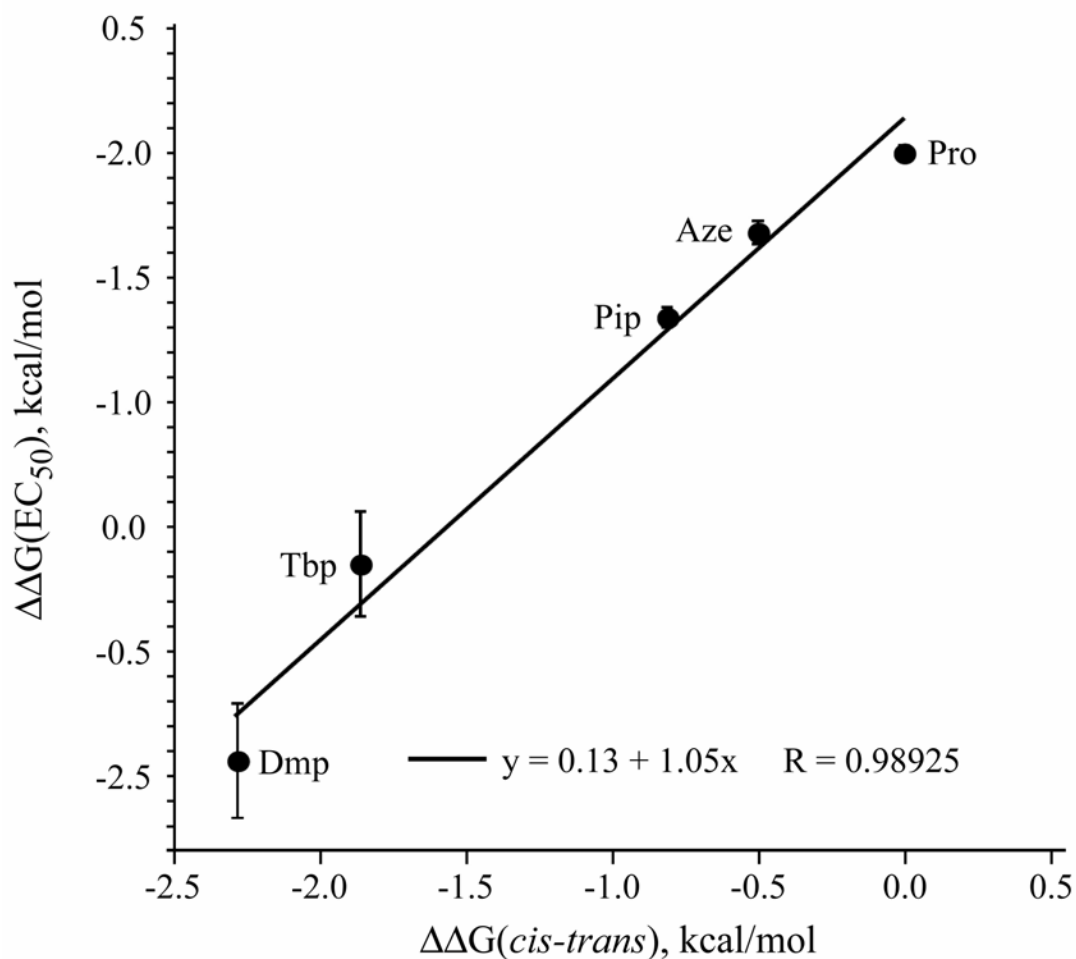


Figure 3.8. Linear free energy correlation between *cis-trans* isomerization and receptor activation.

3.3.5 Schild plot analysis for representative proline analogues in the 5-HT_{3A} receptor

It should be appreciated that our functional analysis produces an EC₅₀ value which reflects the combination of binding and gating events. Schild analysis was performed to validate that the changes in EC₅₀ values upon substitution of Pro 308 with proline analogs was due to a change in gating and not antagonist binding affinity. Schild plots were generated using the competitive antagonist MDL72222 (figure 3.9(A)) in wild type 5-HT_{3A} and in mutant 5-HT_{3A} channels where Pro 308 was substituted with either pipecolic acid (Pip) or 5,5-dimethyl-L-proline (Dmp). The choice of proline analogs was such that it represents a range of *cis* preference (< 0.1% to 71%). Figure 3.9(B) shows a dose response curve of serotonin, in the presence of increasing concentrations of MDL72222 for the wild type 5-HT_{3A}. EC₅₀ values (in nM units) determined at each concentration of MDL72222

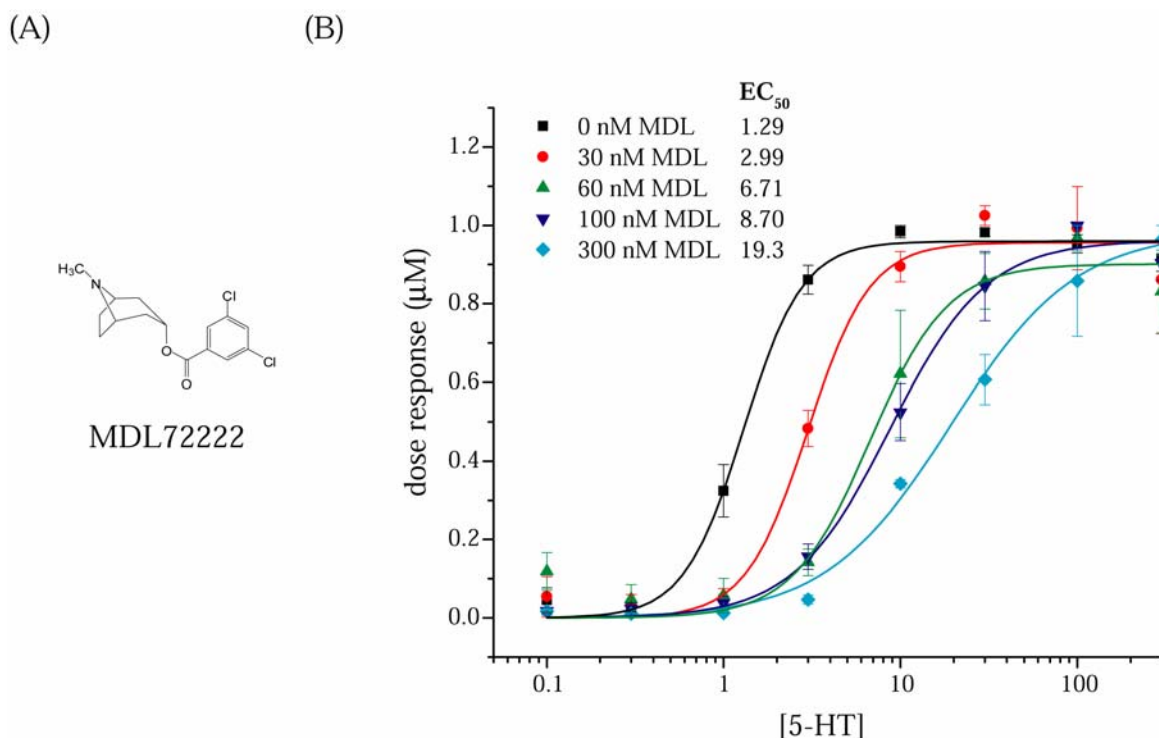


Figure 3.9. (A) Chemical structure of MDL72222, a 5-HT_{3A} receptor antagonist. (B) Dose response curves for wild type 5-HT_{3A} receptor at varying concentrations of MDL72222.

were: 1.29 ± 0.08 (0 nM of MDL72222), 2.99 ± 0.33 (30 nM of MDL72222), 6.70 ± 1.21 (60 nM), 8.69 ± 0.86 (100 nM), and 19.29 ± 2.21 (300 nM). Similar dose response data were generated for receptors containing Pip substituted at Pro 308. EC₅₀ values for receptors containing Pip were: 0.64 ± 0.20 (0 nM of MDL72222), 1.07 ± 0.19 (30 nM of MDL72222), 2.59 ± 0.08 (60 nM of MDL72222), 3.18 ± 0.31 (100 nM of MDL72222), and 5.77 ± 1.3 (300 nM of MDL72222).

The dose response data were used to generate Schild plots (figure 3.10), both of which showed slopes not significantly different from 1. Similar K_d values for MDL72222

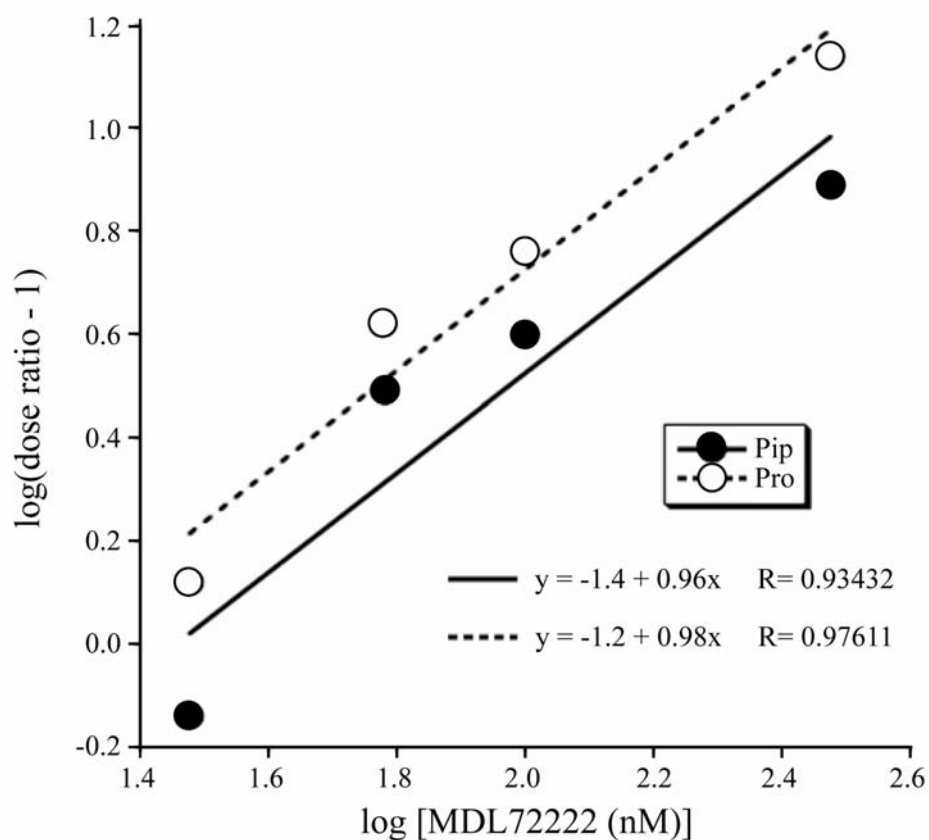


Figure 3.10. Schild Plots for mutant 5-HT_{3A}receptor containing Pip and wild type 5-HT_{3A}receptor.

were obtained for both the wildtype receptor and receptors containing Pip. K_d values were calculated from the x -intercepts to be 18.1 nM for the wild type and 28.9 nM for Pip. MDL72222 IC_{50} values were obtained for the wild type receptor, the Pip containing receptor, and the Dmp containing receptor at their respective EC_{50} values (obtained with serotonin). MDL72222 IC_{50} values determined for the wild type and Pip containing receptors were similar to the obtained MDL72222 K_d values. The MDL72222 IC_{50} values were determined to be 25.9 nM for the wild type receptor and 20.6 nM for the Pip containing channel. The determined IC_{50} value for Dmp, at its EC_{50} value, was also similar to that of the wild type and was determined to be 44.7 nM. The plot of the pIC_{50} at the respective EC_{50} , against the $-\log(EC_{50})$ showed a slope that does not deviate significantly from zero (figure 3.11).

3.3.6 Electrophysiological analysis for substitution of at site 265 and site 272 of the alpha subunit of the nicotinic acetylcholine receptor

Conventional mutagenesis was used to generate mutants in which the proline at either site 265 or site 272 of the alpha subunit of the nicotinic acetylcholine receptor was substituted to glycine, alanine or valine. Sites 265 and 272 are analogous to proline 301 and 308, respectively of the 5-HT_{3A} receptor. Corresponding messenger RNA was transcribed and subsequently injected into *Xenopus* oocytes for functional analysis using two-electrode voltage clamp electrophysiology. Conventional mutants were used initially to determine if either proline is necessary to produce functional channels.

Interestingly, substitutions at site 265 in the alpha subunit of the nicotinic acetylcholine receptor were not tolerated and none of the three mutant receptors showed channel activity. This result was unanticipated since the analogous site in the 5-HT_{3A}

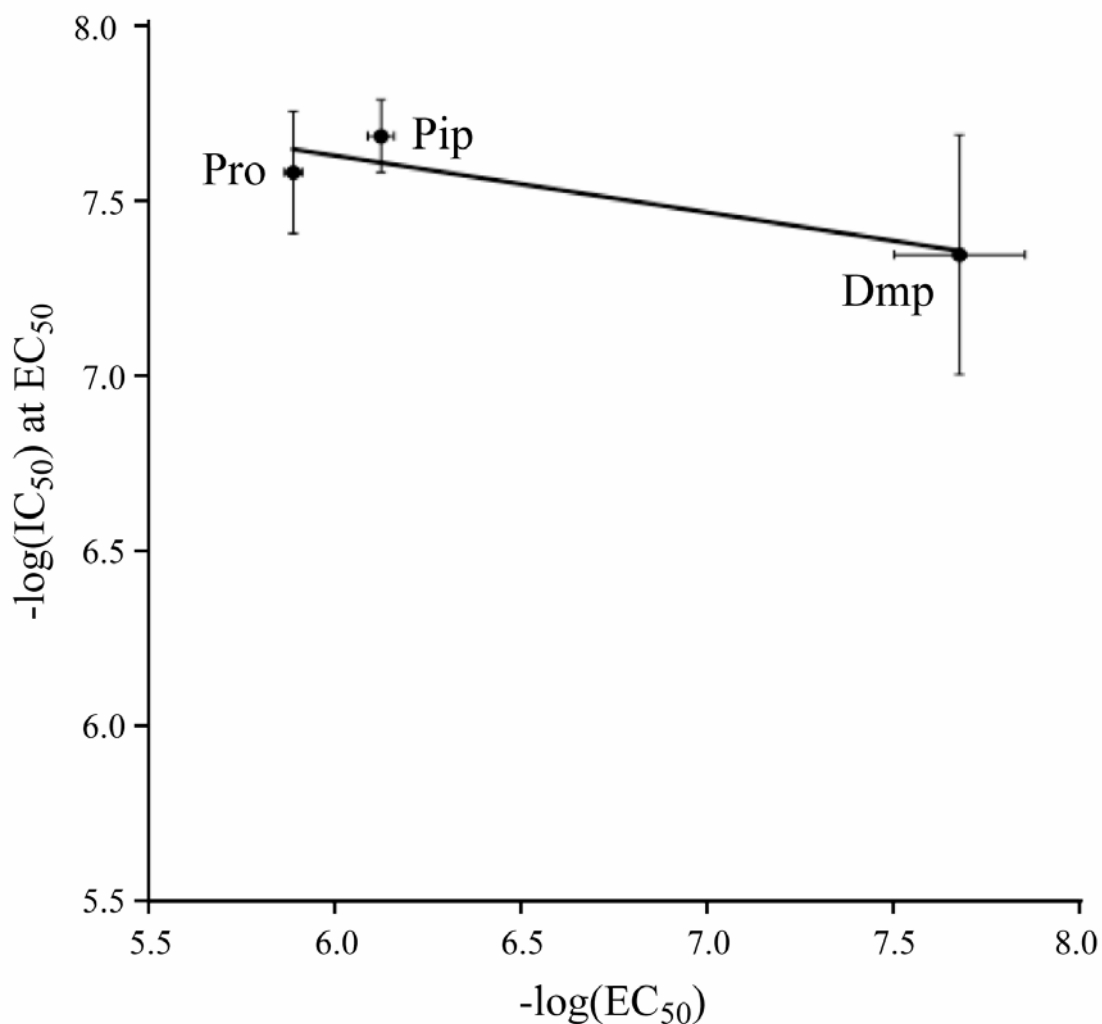


Figure 3.11. pIC₅₀ values (at the respective EC₅₀) plotted against $-\log(\text{EC}_{50})$ for Schild Plot for wild type 5-HT_{3A} receptor and mutant 5-HT_{3A} receptors containing Pip or Dmp.

receptor (Pro 301) was shown to be promiscuous and a variety of substitutions produced functional receptors. Conversely, substitutions at site 272 (analogous to Pro 308 of the 5-HT_{3A} receptor) appear to be well tolerated. EC₅₀ values for the alanine and glycine mutant receptors showed no significant difference from that obtained for the wild type receptor.

3.4 Discussion

3.4.1 *Cis-trans* isomerization of Proline 308 in the gating of 5-HT_{3A} receptor

A series of proline analogs were substituted at site 308 of the 5-HT_{3A} receptor using nonsense suppression methodology in a *Xenopus* oocyte expression system. Functional analysis was performed using two-electrode voltage clamp electrophysiology. Analogs that had a reduced *cis* preference relative to proline, namely 2,4-CH₂-Pro and 2-Me-Pro, produced receptors that were transported to the cell surface, but were nonfunctional. C-4F-Pro and t-4F-Pro, which show similar intrinsic *cis-trans* preferences to proline, produced EC₅₀ values similar to that of the wild-type receptor.

Analysis of EC₅₀ values obtained for proline analogs with a range of *cis-trans* preferences strongly supports a role for *cis-trans* isomerization of proline 308 in the gating of the 5-HT_{3A} receptor. A linear free energy relationship was observed between the intrinsic *cis-trans* energy gap of the proline analog and activation of the receptor. Because EC₅₀ values represent a combination of ligand binding and gating events, Schild analysis was performed to establish that substitutions at site 308 affected gating and not ligand binding affinity. Experimental results from Schild analysis using the competitive antagonist MDL72222 indicate that substitution with amino acids with a range of *cis* preferences does not perturb the binding site. We therefore conclude that the changes in EC₅₀ values, upon substitution at site 308, are due to changes in receptor gating, not binding. Specifically, our experimental data strongly suggest a link between the *cis-trans* isomerization at site 308 (Pro 8*) and the gating of the 5-HT_{3A} receptor.

From these data, we propose a model of gating for the 5-HT_{3A} receptor (figure 3.12). In the closed state of the channel, proline 308 is in the *trans* conformation. Upon ligand

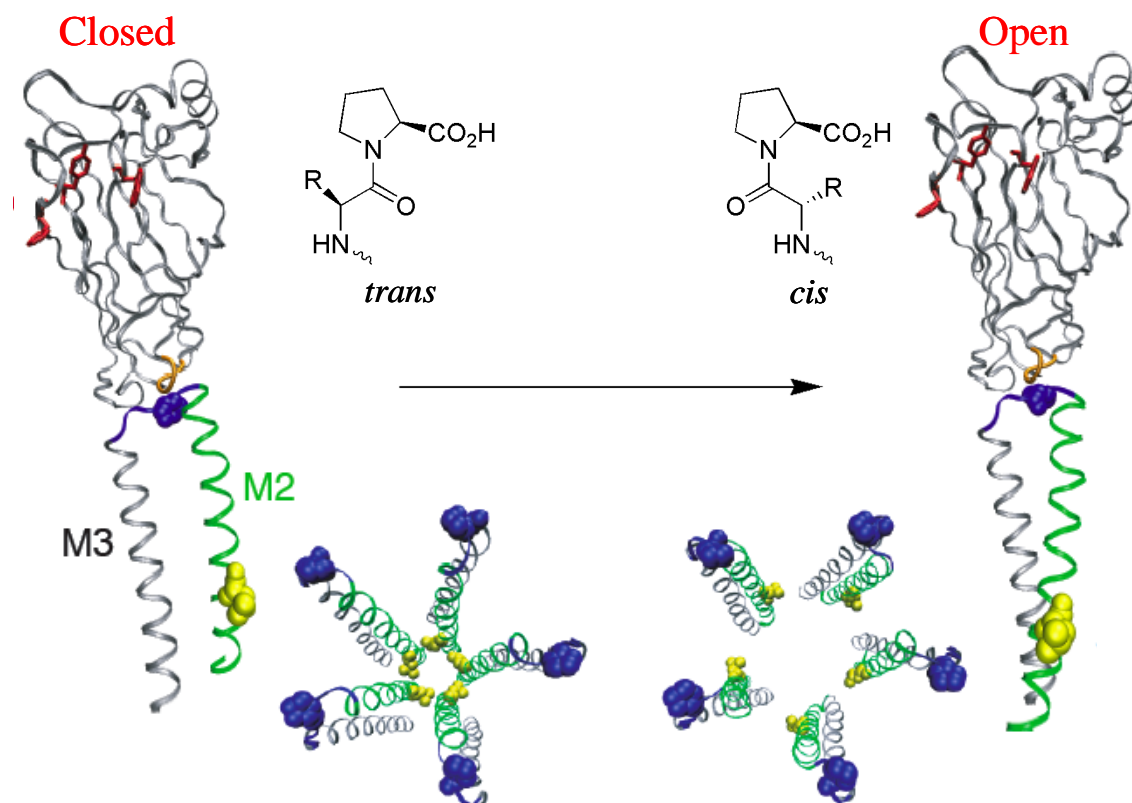


Figure 3.12. Proposed model for the gating mechanism of the 5-HT_{3A} receptor.

binding, a series of conformational changes occurs that results in the isomerization of proline 308 to the *cis* conformation. Proline 308 serves as a hinge point in the M2-M3 loop; isomerization to the *cis* conformation causes a reorientation of the M2 transmembrane helix which opens the channel. Proline 308 is positioned at the apex of the M2-M3 loop and is in close proximity to the extracellular β 1- β 2 loop and the Cys-loop (loops 2 and 7, respectively). As such, it may serve as the link between the ligand binding site and the channel gate. Previous models have proposed that loops 2 and 7 conformationally restrict the M2 helix in the closed state. We expand on this model by proposing that loop 2 and 7 act as “calipers” to hold proline 308 in the *trans* conformation in the closed state. Ligand binding

results in the movement of tryptophan 183, a key tryptophan in the binding site; this movement is propagated such that it releases the clamp on proline 308, which can then undergo *cis-trans* isomerization, gating the channel.

We recognize that the time scale of gating for the 5-HT_{3A} receptor is on the order 10-100 s⁻¹ while the intrinsic rate for the *cis-trans* isomerization of proline has been reported to be roughly ten times slower. This timescale difference can be reconciled if we consider the possibility that structural features of the receptor may accelerate the isomerization rate. Proline *cis-trans* isomerization is widely accepted as the rate limiting step in protein folding, and these processes can be significantly accelerated by protein prolyl isomerases. Furthermore, it has been demonstrated that a hydrogen bond to the proline amide nitrogen can accelerate the isomerization rate roughly 260-fold. Therefore, it is possible that the 5-HT_{3A} receptor utilizes structural features to accelerate the isomerization of proline 308.

3.4.2 Studies of proline 1* and 8* of the alpha subunit of nAChR

We extended our studies to the nicotinic acetylcholine receptor to examine if the *cis-trans* isomerization of the analogous proline plays a role in channel gating. Functional analysis of mutant receptors of Proline 265 (Pro 1*), in the alpha subunit of the nicotinic acetylcholine receptor, containing glycine, alanine or valine suggested that mutations at this site are not tolerated. None of the mutant receptors showed channel activity. These results are in contrast to those found with substitutions at the analogous proline site (site 301) in the 5-HT_{3A} receptor, which appeared to be well tolerated.

Replacement of proline 272, which is analogous to proline 265 in the 5-HT_{3A} receptor, with glycine or alanine produced receptors that showed channel activity similar to

wild type activity (data not shown). EC_{50} values for the mutant receptors did not deviate significantly from that obtained for the wild type receptor. This was an unanticipated result since comparable mutations in the analogous site in the 5-HT_{3A} receptor produced non-functional channels. Our initial results suggest that proline 272 of the nicotinic acetylcholine receptor does not play a significant role in channel gating. This is interesting because it suggests that these channels have evolved to utilize different mechanisms of gating despite being highly homologous and being members of the same superfamily. This work was done in the muscle type nicotinic receptor which exhibits faster kinetics than that of the neuronal subtype receptor, which may account for the differences in experimental observations. Similar studies in a neuronal subtype of the nicotinic acetylcholine receptor are now underway.

3.5 Conclusions

A series of proline analogues, of varying *cis* preference were incorporated at proline 308 in the M2-M3 loop of the 5-HT_{3A} receptor to examine the possible role of *cis-trans* isomerization in the gating of the channel. *In vivo* nonsense suppression methodology was used to incorporate these proline analogs in a *Xenopus* oocyte expression system. Electrophysiological analysis of the mutant channels was used to generate dose-response curves and determine an EC_{50} for each mutant channel. Data show a linear relationship between the *cis* preference of the proline analog and the EC_{50} of the mutant channel—suggesting that proline 308 may serve as a hinge during the gating 5-HT_{3A}. Schild plots were generated to validate that the shifts in EC_{50} were due to changes in channel gating and not

changes in agonist binding affinity. From these data, we proposed a model of gating for the 5-HT_{3A} receptor.

Initial studies were also done on the analogous prolines in the nicotinic acetylcholine receptor to examine if these prolines are critical for channel function. Conventional mutagenesis was performed on prolines 265 and 272 to generate glycine, valine and alanine mutants. Mutations of proline 272 (analogous to proline 308 in 5-HT_{3A}R) of the alpha subunit of nAChR produced functional channels. Furthermore, incorporation of Aze and Pip using nonsense suppression at proline 272 yielded EC₅₀ values on the same order of magnitude as wildtype channels. Interestingly, mutations at proline 265 of nAChR were not tolerated and yielded no channel activity. Proline 301 of 5-HT_{3A} was previously shown to tolerate mutations. Our initial data suggest that while proline 8* is involved in gating of 5-HT_{3A} receptors, it does not play the same role in nAChR; however, proline 1* in the alpha subunit of nAChR may play a critical role in gating although the equivalent proline does not appear to play a role in 5-HT_{3A} gating. These data are interesting because they suggest that these two channels have evolved to utilize different gating mechanisms despite being highly homologous and part of the same superfamily. The observed difference may also be due to the kinetics of the muscle type nAChR since the initial studies were done in the mouse muscle type receptor. To address this issue, these studies are being continued by Joanne Xiu in a neuronal nACh receptor.

3.6 *Experimental method and materials*

3.6.1 *General synthetic information*

Unless otherwise stated, all reactions were performed in flame-dried glassware under an atmosphere of nitrogen gas or argon gas. Reagents were obtained from commercial sources and used as received. Thin-layer chromatography (TLC) was performed using E. Merck silica gel 60 F254 precoated plates (0.25 mm). Visualization of the developed chromatogram was performed by fluorescence quenching, cerium ammonium molybdate stain, ninhydrin stain, or basic potassium permanganate stain. Chromatography (flash) was performed using ICN Silica gel (0.032-0.063 mm) or Fluka alumina oxide type 507 C neutral (0.05-0.15 mm). $^1\text{H-NMR}$ and $^{13}\text{C-NMR}$ were recorded on a Varian Mercury 300 (300 MHz for $^1\text{H-NMR}$ and 74.5 MHz for $^{13}\text{C-NMR}$) at room temperature. Infrared (IR) spectra were obtained using a Perkin Elmer Paragon spectrometer and are reported in terms of frequency of absorption (cm^{-1}). UV (vis) spectra were recorded on a Unikon Spectrophotometer 930 and are reported in terms of wavelength of maximum absorbance (λ_{max}). Mass spectra were obtained from the Protein/Peptide MicroAnalytical Laboratory at the California Institute of Technology, Pasadena, California.

3.6.2 *Synthesis of (2S,5R)-5-tert-Butylproline*

3.6.2.1 *N-(9-(9-Phenylfluorenyl))glutamic Acid γ -Methyl Ester (2)*

To a suspension of glutamic acid γ -methyl ester **1** (4.06 g, 25.2 mmol) in freshly distilled chloroform (50.4 mL) was added chlorotrimethylsilane (TMS-Cl) (2.88 g, 3.36 mL) via syringe at room temperature. The reaction mixture was heated at reflux for 2 h. and cooled to room temperature. Freshly distilled triethylamine (7.39 mL) was added followed

by lead nitrate (5.01 g, 15.13 mmol) and 9-bromo-9-phenylfluorene (9.71 g, 30.23 mmol) in chloroform (50.4 mL). The resulting mixture was stirred for 87 h. at room temperature, after which dry methanol (16.8 mL) was added and the reaction was stirred for another 15 minutes. The solution was filtered by vacuum filtration and the filtrate was concentrated *in vacuo*. The resulting residue was dissolved in 5% citric acid (84 mL) and extracted three times with ethyl acetate (3 x 84 mL). The combined organic layers were dried with anhydrous sodium sulfate (granular), filtered and concentrated *in vacuo*. Column chromatography on silica gel (gradient 1:1 EtOAc: Hexanes to 2:1 EtOAc: Hexanes) yielded a yellow residue (85 % yield). ^1H NMR (300 MHz, CDCl_3) δ = 1.58-1.81 (2H, m), 2.31 (2H, t, J = 6.9), 2.56 (1H, dd, J = 4.8, J = 7.5), 3.58 (3H, s), 6.00 (1H, bs), 7.10-7.61 (13H, m). ^{13}C NMR (300 MHz, CDCl_3) δ = 28.11, 30.49, 52.07, 55.55, 73.05, 74.06, 120.30, 120.42, 125.34, 126.17, 126.29, 127.76, 128.05, 128.33, 128.73, 128.99, 129.14, 140.59, 141.20, 143.66, 147.44, 151.08, 159.78, 174.61, 177.98. MS Calcd for $\text{C}_{25}\text{H}_{23}\text{NO}_4$ = 401.16. Found: (ESI $^+$) 402.2 $[\text{M} + \text{H}]^+$, 424.0 $[\text{M} + \text{Na}]^+$

3.6.2.2 (2*S*, 4*RS*)-6,6-dimethyl-5-oxo-4-[(methoxy)carbonyl]-2-[(*N*-(PhF)amino)hepantoic acid (**3**)

To a -78 °C solution of 1 M lithium bis(trimethylsilyl)amide (12.35 mL), is added dropwise **2** (1.5 g, 3.74 mmol) dissolved in dry tetrahydrofuran (THF) (4.78 mL) that has been cooled to -78 °C. The reaction mixture is stirred at -78 °C for 2 h. to generate the enolate. To the enolate is added dropwise a -78 °C solution of trimethylacetylchloride (pivaloyl chloride) (1.29 mL) in dry tetrahydrofuran (THF) (0.875mL). The reaction mixture is stirred at -78 °C for 1 h, after which 1 M sodium dihydrogen phosphate (NaH_2PO_4) is

added. The reaction is allowed to come to room temperature with stirring. The reaction is then extracted with ethyl acetate (4 x 7.3 mL), and the combined organic layers are washed with cold water (3 x 2.9 mL) and brine (2 x 4.35 mL), dried with anhydrous sodium sulfate (granular), filtered and concentrated *in vacuo* to yield an orange residue (75% yield). The residue is used without further purification in the next reaction.

3.6.2.3 (2S)-6,6-dimethyl-5-oxo-2-[N-(PhF)amino heptanoic acid

Crude β -keto ester **3** (diastereomers, 1.36 g, 2.81 mmol scale) from the previous reaction was dissolved in 200 proof ethanol (18.2 mL) and treated with 2N NaOH (18.2 mL) and stirred under reflux for 48 h. The reaction was cooled to room temperature and the pH was adjusted to 5 using 10% aqueous HCl. The solution was extracted with ethyl acetate (three times), dried with anhydrous sodium sulfate (granular), filtered, and concentrated *in vacuo* to yield a light yellow residue. The product did not require further purification and was used in the next reaction. $^1\text{H NMR}$ (300 MHz, CDCl_3) δ = 1.12 (9H, s), 1.61-1.84 (2H, m), 2.51 (2H, m), 2.61 (1H, dd, J = 5.1, J = 6.6), 7.23-7.73 (13H, m). MS Calcd for $\text{C}_{28}\text{H}_{29}\text{NO}_3$ = 427.53. Found: (ESI $^+$) 428.2 [M + H] $^+$.

3.6.2.4 (2S)-methyl 6,6-dimethyl-5-oxo-2-[N-(PhF)amino heptanoic acid (**4**)

Crude acid (2S)-6,6-dimethyl-5-oxo-2-[N-(PhF)amino heptanoic acid (from previous reaction) was dissolved in dry acetonitrile (2.77 mL) and to that was added K_2CO_3 (0.947 g, and methyl iodide (0.728 mL) and stirred at room temperature for 19 h. Brine was added to the reaction mixture and then the reaction mixture was extracted with ethyl acetate (3 x 15 mL). The combined organic phases were washed with 0.65M sodium thiosulfate (29.1 mL)

and then brine. It was then dried with anhydrous sodium sulfate (granular), filtered and concentrated *in vacuo*. Column chromatography on silica gel (1:9 ethyl acetate:hexanes) yielded a white powder (78% for two steps). ^1H NMR (300 MHz, CDCl_3) δ = 1.11 (9H, s), 1.62 (2H, m), 2.31 (1H, ddd, J = 6.0, J = 9.3, J = 18), 2.53 (1H, dd, J = 5.4, J = 7.5), 2.72 (1H, ddd, J = 5.7, J = 9.5, J = 18), 3.00 (1H, bs), 3.27 (3H, s), 7.16 – 7.70 (13H, m). ^{13}C NMR (300 MHz, CDCl_3) δ = 14.41, 26.75, 29.31, 33.29, 44.21, 51.74, 55.21, 120.11, 120.26, 125.50, 126.25, 126.47, 127.46, 127.53, 127.96, 128.52, 128.59, 140.33, 141.31, 144.63, 148.75, 149.28, 176.77. MS Calcd for $\text{C}_{29}\text{H}_{31}\text{NO}_3$ = 441.56. Found: (ESI⁺) 442.2 [M + H]⁺, 464.0 [M + Na]⁺, 480.0 [M + K]⁺.

3.6.2.5 (2*S*,5*R*)-*N*-(*BOC*)-5-*tert*-Butylproline Methyl Ester (5)

A solution of **4** (1.30 g, 2.94 mmol) and di-*tert*-butyldicarbonate (1.77 g, 8.11 mmol) in anhydrous methanol (89.4 mL) was treated with 10% palladium-on-carbon (239.6 mg) and stirred under 4 atm (58 psi) of hydrogen using a par hydrogenator for 48 h. The mixture was filtered through Celite and washed with methanol and the filtrate was concentrated *in vacuo*. Column chromatography on silica (0 to 25% EtOAc in Hexanes) yielded a white crystalline solid (71% yield). ^1H NMR (300 MHz, CDCl_3) δ = 0.95 (9H, s), 1.43 (9H, s), 1.95 (3H, m), 2.27 (1H, m), 3.70 (3H, s), 3.77 (1H, d, J = 8.1), 4.27 (1H, m). ^{13}C NMR (300 MHz, CDCl_3) δ = 26.85, 27.63, 28.43, 29.82, 36.55, 52.00, 61.70, 66.82, 80.13, 155.90, 173.70. MS Calcd for $\text{C}_{15}\text{H}_{27}\text{NO}_4$ = 285.38. Found: (ESI⁺) 286.2 [M + H]⁺, 308.1 [M + Na]⁺, 324.1 [M + K]⁺ [α]_D^{23.4} -31.5 (c 1, MeOH).

3.6.2.6 (2*S*,5*R*)-*N*-(*BOC*)-5-*tert*-Butylproline (6)

Methyl ester *cis*-**5** (187 mg, 0.655 mmol) was dissolved in diethyl ether (4.6 mL) and treated with potassium trimethylsilanolate (KOSiMe₃) (93.5 mg, 0.729 mmol) and stirred at room temperature for 22 h after which another portion of potassium trimethylsilanolate (93.5 mg, 0.729 mmol) was added and the reaction was stirred for another 2 h. The reaction was concentrated *in vacuo* and the residue was redissolved in 5% citric acid (40 mL). The solution was extracted with ethyl acetate (3 x 25 mL). The combined organic layers were washed with brine, dried with anhydrous sodium sulfate (granular), filtered and concentrated *in vacuo* to yield the desired product (quant. yield). No further purification was necessary. ¹H NMR (300 MHz, CDCl₃) δ = 0.95 (9H, s), 1.43 (9H, s), 1.95 (3H, m), 2.28 (1H, m), 3.78 (1H, d, *J* = 7.8), 4.28 (1H, m). ¹³C NMR (300 MHz, CD₃OD) δ = 27.71, 28.12, 28.71, 30.80, 37.38, 62.81, 68.32, 81.44, 158.00, 176.86. MS Calcd for C₁₄H₂₅NO₄ = 271.35. Found: (ESI⁺) 272.1 [M + H]⁺, 294.0 [M + Na]⁺, 310.0 [M + K]⁺, 316.0 [M + 2Na - H]⁺, 332.0 [M + K + Na - H]⁺.

3.6.2.7 (2*S*,5*R*)-5-*tert*-Butylproline (**6**)

A solution of (2*S*,5*R*)-N-(BOC)-5-*tert*-Butylproline **6** (189.58 mg, 0.699 mmol) in anhydrous CH₂Cl₂ (20 mL) was treated with trifluoroacetic acid (1 mL) and stirred at room temperature for 12 h. The reaction was concentrated *in vacuo* to yield (2*S*,5*R*)-5-*tert*-Butylproline trifluoroacetate salt. No purification was necessary and material was used in next reaction as is. ¹H NMR (300 MHz, CDCl₃) TFA salt δ = 1.08 (9H, s), 1.65 (1H, m), 2.05 (1H, m), 2.41 (2H, m), 3.52 (1H, m), 4.38 (1H, bs), 6.51 (1H, bs), 10.66 (1H, bs). ¹³C NMR (300 MHz, CDCl₃) δ = 25.28, 26.16, 29.29, 32.27, 59.25, 72.40, 172.79. MS Calcd for C₉H₁₇NO₂ = 171.24. Found: (ESI⁺) 172.0 [M + H]⁺, 194.0 [M + Na]⁺.

3.6.2.8 (2S,5R)-N-(NVOC)-5-tert-Butylproline (**8**)

(2S,5R)-5-tert-Butylproline **7** (53.7 mg, 0.314 mmol) was added to 10% sodium carbonate (1.20 mL). Another equivalent of Na₂CO₃ (120 mg) was added to account for the TFA. To this was added dioxane (0.91 mL) and the reaction was cooled to 0 °C (ice bath). NVOC-Cl (90.9 mg, 0.330 mmol) was added slowly to the reaction at 0 °C. The reaction mixture was removed from the ice bath and allowed to warm to room temperature and stirred at room temperature for 4 h. Subsequently, the reaction was poured over water then washed with diethyl ether (3 x). The aqueous layer was acidified to pH 2 with 6 N HCl. Upon acidification, the aqueous layer becomes opaque as product begins to precipitate. The aqueous layer is extracted with methylene chloride (3 x or until the aqueous layer is no longer orange). The combined organic layers were dried with anhydrous sodium sulfate (granular), filtered and concentrated *in vacuo* to yield an orange residue (75% yield). No further purification was necessary and residue was used in next reaction.

3.6.2.9 (2S,5R)-N-(NVOC)-5-tert-Butylproline Cyano-Methyl Ester (**9**)

(2S,5R)-N-(NVOC)-5-tert-Butylproline **8** (128.9 mg, 0.314 mmol) was dissolved in anhydrous chloroacetonitrile (1.19 g, 15.7 mmol, 0.993 mL) and to that was added freshly distilled triethylamine (95.4 mg, 0.942 mmol, 0.131 mL). The reaction was stirred at room temperature until reaction was complete as monitored by thin layer chromatography. The reaction was concentrated *in vacuo* to yield an orange residue. Column chromatography on silica gel (1:2 Ethyl acetate: Hexanes) yielded the desired product (49% yield). ¹H NMR (600 MHz, CDCl₃, 22 °C) δ = 0.91 (9H, s), 1.93 (2H, m), 2.01 (1H, m), 2.36 (1H, m), 3.91

(3H, s), 3.92 (1H, m), 4.03 (3H, s), 4.50 (1H, t, $J = 9, 9.6$), 4.76 (2H, abx pattern*, $J = 16.2, 15.6$), 5.52 (2H, ab pattern, $J = 15.3$), 7.00 (1H, s), 7.68 (1H, s). ^{13}C NMR (300 MHz, CDCl_3) $\delta = 26.60, 27.45, 29.89, 36.51, 48.94, 56.52, 56.96, 60.81, 64.61, 67.99, 108.27, 109.69, 110.89, 114.19, 128.92, 139.32, 148.09, 154.18, 155.95, 171.86$. MS Calcd for $\text{C}_9\text{H}_{17}\text{NO}_2 = 449.45$. Found: (ESI⁺) 472.0 $[\text{M} + \text{Na}]^+$, 487.8 $[\text{M} + \text{K}]^+$.

*at -10 °C: 4.745 (2H, abx, $J_{\text{AB}} = 25.2, J_{\text{BX}} = 15.6, J_{\text{AB}} = 22.8, J_{\text{AX}} = 15.6$)

CALIFORNIA INSTITUTE OF TECHNOLOGY
BECKMAN INSTITUTE
X-RAY CRYSTALLOGRAPHY LABORATORY

Date 15 December 2004

Crystal Structure Analysis of:

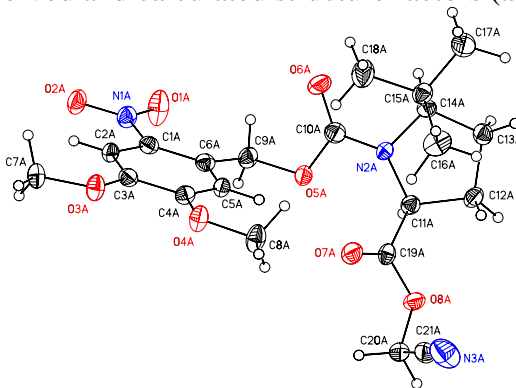
LWL01

(shown below)

For Investigator: Lori Lee ext. 6009
Advisor: D. A. Dougherty ext. 6089
Account Number: DAD.00007-1-NIH.000076
By Michael W. Day 116 Beckman ext. 2734
e-mail: mikeday@caltech.edu

Contents

- Table 1. Crystal data
- Figures Figures
- Table 2. Atomic Coordinates
- Table 3. Full bond distances and angles
- Table 4. Anisotropic displacement parameters
- Table 5. Hydrogen atomic coordinates
- Table 6. Observed and calculated structure factors (available upon request)



LWL01

Note: The crystallographic data have been deposited in the Cambridge Database (CCDC) and has been placed on hold pending further instructions from me. The deposition number is 258350. Ideally the CCDC would like the publication to contain a footnote of the type: "Crystallographic data have been deposited at the CCDC, 12 Union Road,

Cambridge CB2 1EZ, UK and copies can be obtained on request, free of charge, by quoting the publication citation and the deposition number 258350."

Table 3.2. Crystal data and structure refinement for LWL01 (CCDC 258350).

Empirical formula	C ₂₁ H ₂₇ N ₃ O ₈	
Formula weight	449.46	
Crystallization Solvent	Ethylacetate	
Crystal Habit	Block	
Crystal size	0.30 x 0.28 x 0.26 mm ³	
Crystal color	Yellow	
Data Collection		
Type of diffractometer	Bruker SMART 1000	
Wavelength	0.71073 Å MoK α	
Data Collection Temperature	100(2) K	
θ range for 12341 reflections used in lattice determination	2.24 to 27.04°	
Unit cell dimensions	a = 8.6423(8) Å b = 26.431(2) Å c = 9.7211(8) Å	β = 96.1050(10)°
Volume	2208.0(3) Å ³	
Z	4	
Crystal system	Monoclinic	
Space group	P2 ₁	
Density (calculated)	1.352 Mg/m ³	
F(000)	952	
Data collection program	Bruker SMART v5.630	
θ range for data collection	1.54 to 28.46°	
Completeness to $\theta = 28.46^\circ$	93.4 %	
Index ranges	-10 \leq h \leq 11, -34 \leq k \leq 35, -12 \leq l \leq 12	
Data collection scan type	ω scans at 5 ϕ settings	
Data reduction program	Bruker SAINT v6.45A	
Reflections collected	31693	
Independent reflections	10131 [R _{int} = 0.0550]	
Absorption coefficient	0.105 mm ⁻¹	
Absorption correction	None	
Max. and min. transmission	0.9733 and 0.9693	

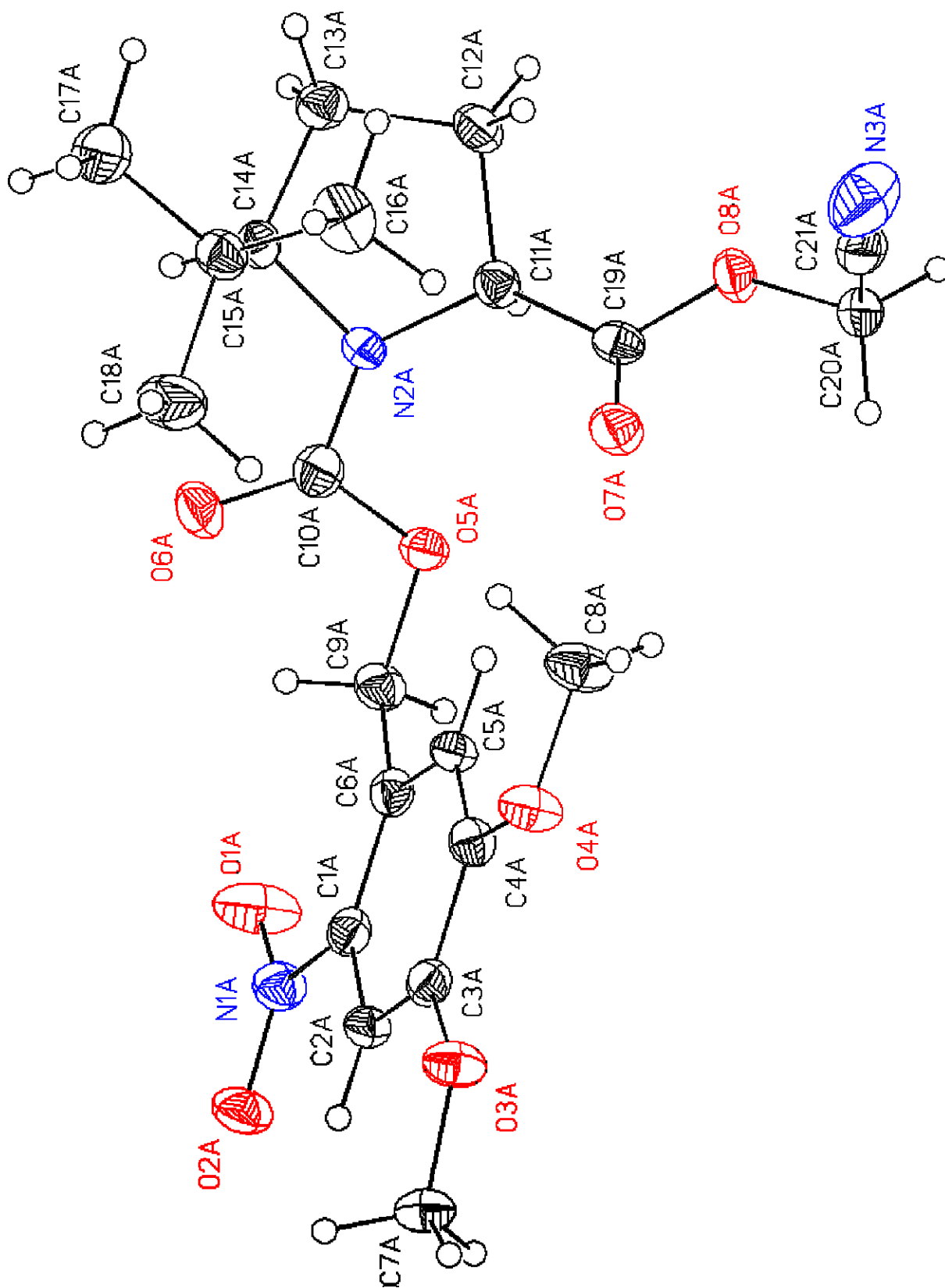
Table 3.2 (cont.)

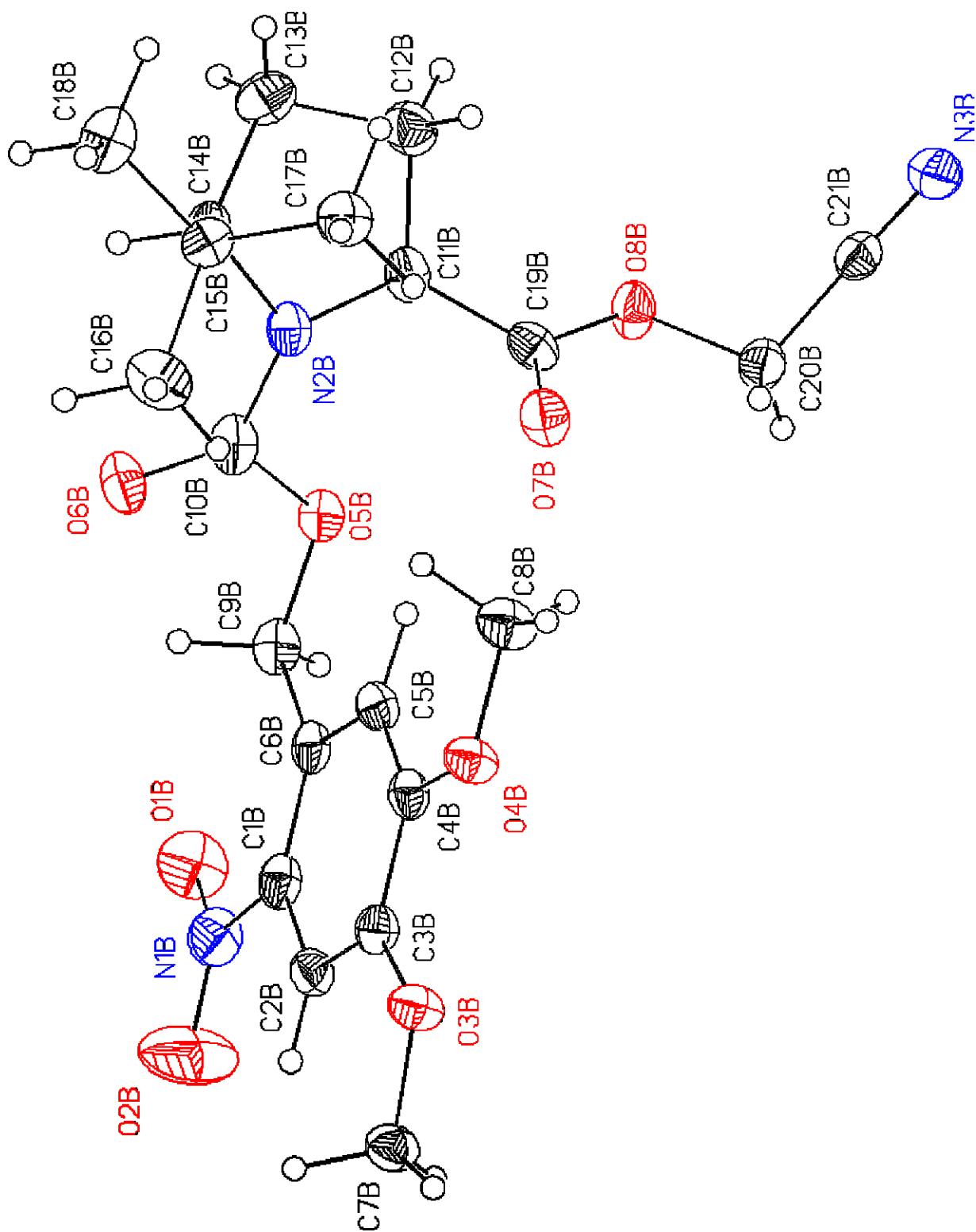
Structure solution and Refinement	
Structure solution program	SHELXS-97 (Sheldrick, 1990)
Primary solution method	Direct methods
Secondary solution method	Difference Fourier map
Hydrogen placement	Difference Fourier map
Structure refinement program	SHELXL-97 (Sheldrick, 1997)
Refinement method	Full matrix least-squares on F^2
Data / restraints / parameters	10131 / 1 / 793
Treatment of hydrogen atoms	Unrestrained
Goodness-of-fit on F^2	1.101
Final R indices [$I > 2\sigma(I)$, 7697 reflections]	$R1 = 0.0373$, $wR2 = 0.0536$
R indices (all data)	$R1 = 0.0566$, $wR2 = 0.0564$
Type of weighting scheme used	Sigma
Weighting scheme used	$w=1/\sigma^2(F_o^2)$
Max shift/error	0.002
Average shift/error	0.000
Absolute structure parameter	0.4(5) Can not be reliably determined for light atom structures.
Largest diff. peak and hole	0.185 and -0.179 e.Å ⁻³

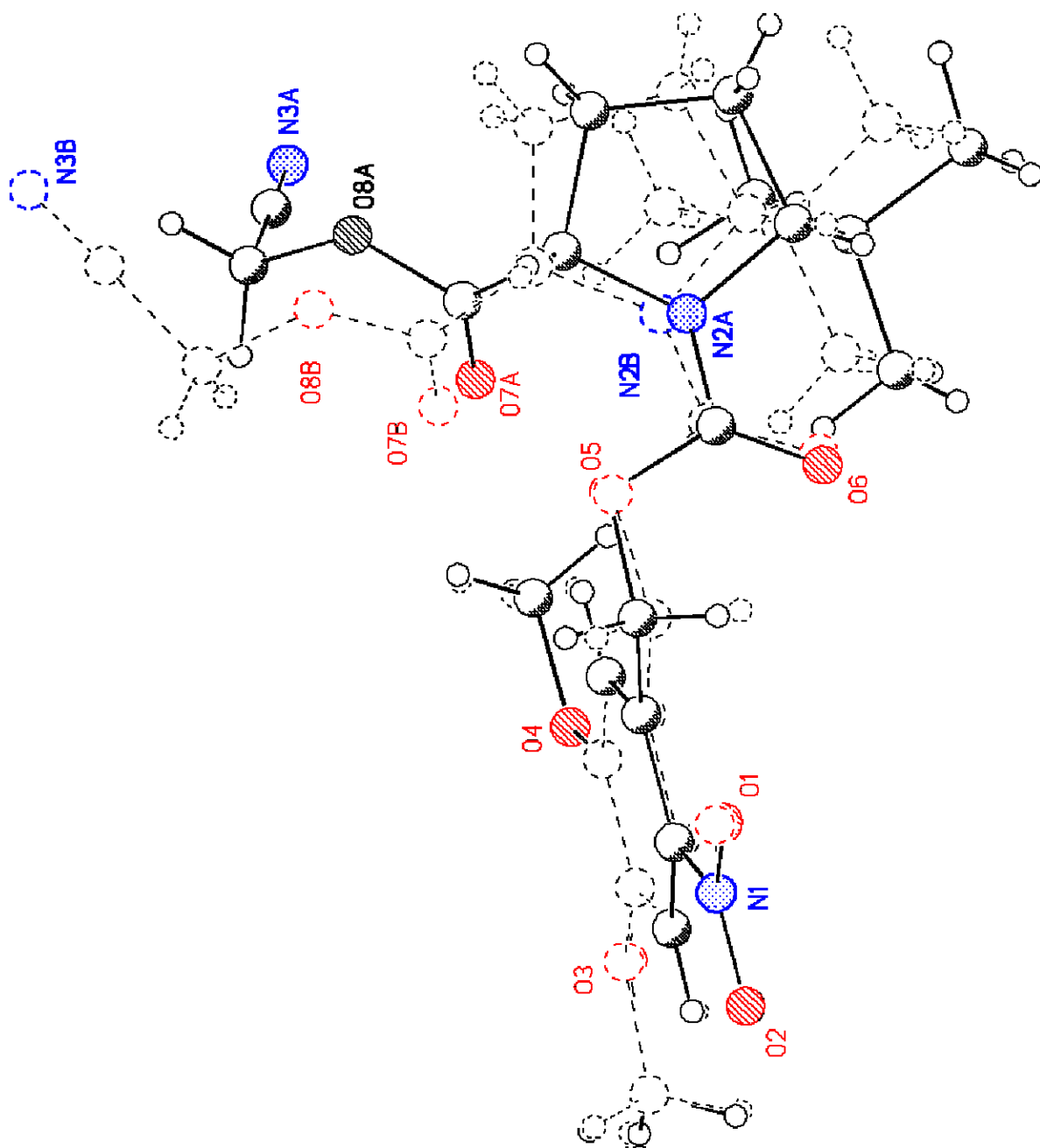
Special Refinement Details

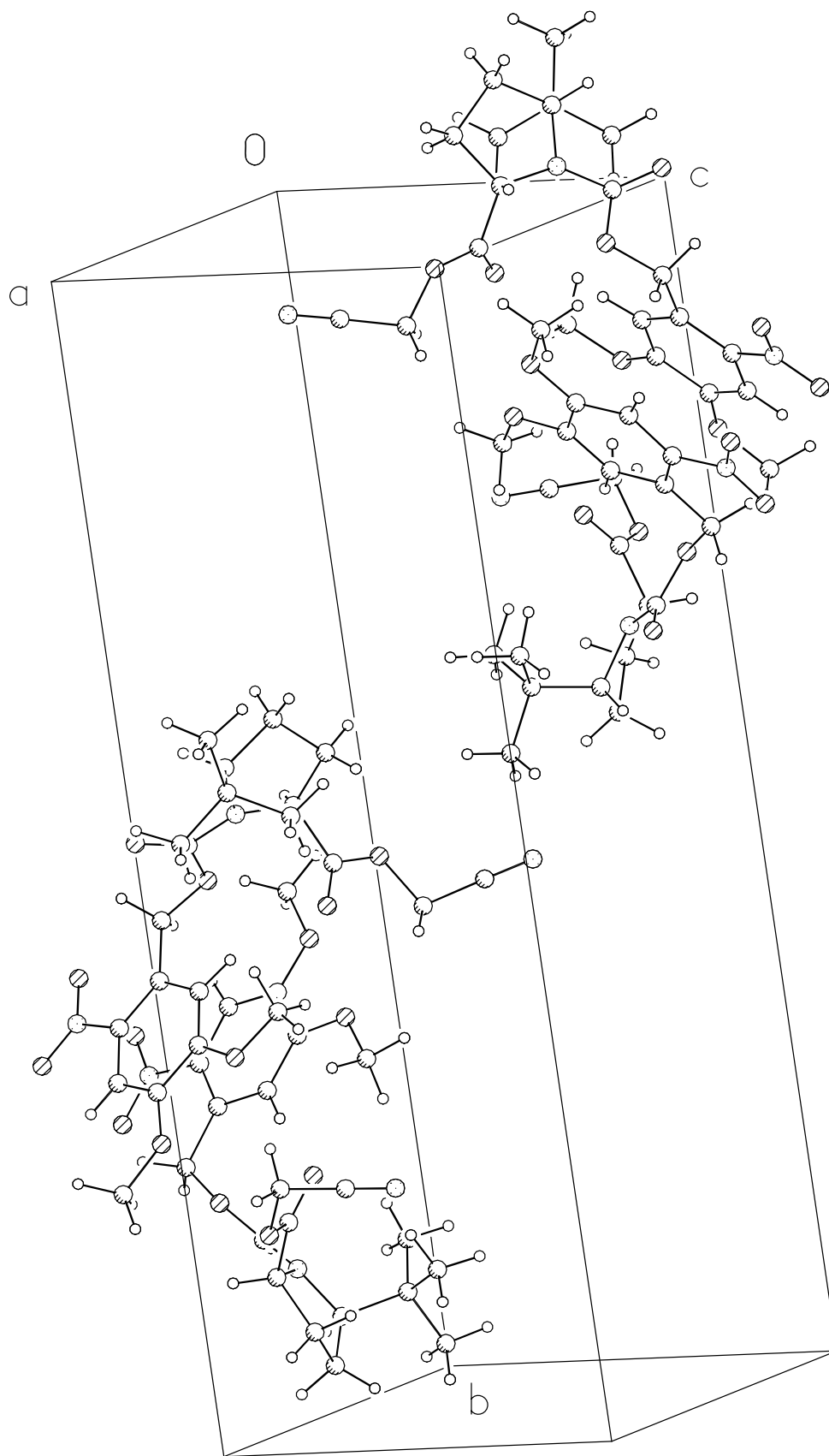
Refinement of F^2 against ALL reflections. The weighted R-factor (wR) and goodness of fit (S) are based on F^2 , conventional R-factors (R) are based on F , with F set to zero for negative F^2 . The threshold expression of $F^2 > 2\sigma(F^2)$ is used only for calculating R-factors(gt) etc. and is not relevant to the choice of reflections for refinement. R-factors based on F^2 are statistically about twice as large as those based on F , and R-factors based on ALL data will be even larger.

All esds (except the esd in the dihedral angle between two l.s. planes) are estimated using the full covariance matrix. The cell esds are taken into account individually in the estimation of esds in distances, angles and torsion angles; correlations between esds in cell parameters are only used when they are defined by crystal symmetry. An approximate (isotropic) treatment of cell esds is used for estimating esds involving l.s. planes.









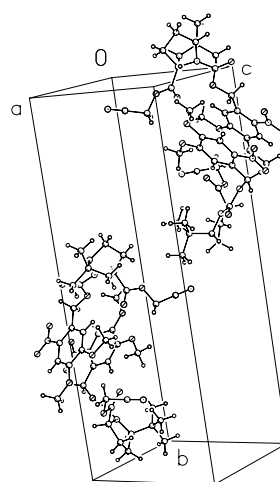
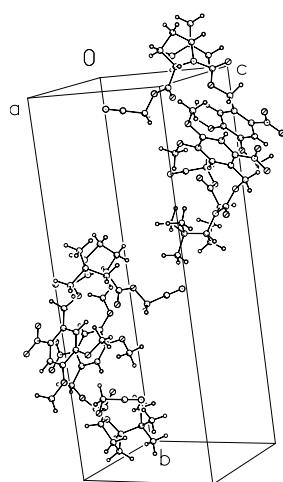


Table 3.3. Atomic coordinates ($\times 10^4$) and equivalent isotropic displacement parameters ($\text{\AA}^2 \times 10^3$) for LWL01 (CCDC 258350). $U(\text{eq})$ is defined as the trace of the orthogonalized U^{ij} tensor.

	x	y	z	U_{eq}
O(1A)	4696(2)	2483(1)	14230(1)	43(1)
O(2A)	6229(2)	1843(1)	14509(1)	31(1)
O(3A)	6527(2)	1098(1)	9861(1)	28(1)
O(4A)	4806(2)	1655(1)	8172(1)	28(1)
O(5A)	2405(1)	3022(1)	10632(1)	22(1)
O(6A)	4504(2)	3534(1)	10757(1)	36(1)
O(7A)	1379(2)	2747(1)	7496(1)	29(1)
O(8A)	-1036(1)	3073(1)	7370(1)	24(1)
N(1A)	5348(2)	2121(1)	13762(2)	25(1)
N(2A)	2583(2)	3616(1)	8993(1)	21(1)
N(3A)	-897(2)	2725(1)	4040(2)	50(1)
C(1A)	5116(2)	2018(1)	12283(2)	21(1)
C(2A)	5937(2)	1605(1)	11827(2)	21(1)
C(3A)	5811(2)	1490(1)	10439(2)	22(1)
C(4A)	4852(2)	1793(1)	9505(2)	21(1)
C(5A)	4049(2)	2196(1)	9991(2)	20(1)
C(6A)	4146(2)	2322(1)	11386(2)	20(1)
C(7A)	7386(3)	750(1)	10778(2)	28(1)
C(8A)	3820(3)	1945(1)	7183(2)	32(1)
C(9A)	3180(2)	2762(1)	11829(2)	24(1)
C(10A)	3267(2)	3406(1)	10174(2)	26(1)
C(11A)	919(2)	3566(1)	8532(2)	21(1)
C(12A)	560(2)	4016(1)	7542(2)	25(1)
C(13A)	1857(2)	4395(1)	7938(2)	24(1)
C(14A)	3288(2)	4079(1)	8461(2)	23(1)
C(15A)	4460(2)	3975(1)	7398(2)	25(1)
C(16A)	3680(3)	3743(1)	6074(2)	36(1)
C(17A)	5215(3)	4478(1)	7079(3)	35(1)
C(18A)	5748(3)	3618(1)	8005(3)	40(1)
C(19A)	512(2)	3076(1)	7771(2)	22(1)
C(20A)	-1614(3)	2645(1)	6559(2)	26(1)
C(21A)	-1201(2)	2691(1)	5135(2)	30(1)
O(1B)	7075(2)	6109(1)	-3713(1)	43(1)
O(2B)	8512(2)	6739(1)	-4103(2)	69(1)
O(3B)	11317(1)	7245(1)	387(1)	27(1)
O(4B)	10593(1)	6587(1)	2149(1)	25(1)
O(5B)	6898(1)	5335(1)	-150(1)	24(1)
O(6B)	8956(2)	4858(1)	-603(1)	31(1)
O(7B)	7178(2)	5569(1)	2991(1)	29(1)

O(8B)	4667(1)	5341(1)	2977(1)	28(1)
N(1B)	8061(2)	6424(1)	-3326(2)	32(1)
N(2B)	7731(2)	4726(1)	1332(2)	24(1)
N(3B)	2749(2)	5548(1)	5735(2)	36(1)
C(1B)	8687(2)	6432(1)	-1873(2)	24(1)
C(2B)	9725(2)	6827(1)	-1481(2)	25(1)
C(3B)	10325(2)	6874(1)	-136(2)	22(1)
C(4B)	9911(2)	6517(1)	837(2)	21(1)
C(5B)	8882(2)	6133(1)	432(2)	22(1)
C(6B)	8240(2)	6076(1)	-940(2)	22(1)
C(7B)	11695(3)	7632(1)	-556(2)	28(1)
C(8B)	10226(3)	6240(1)	3197(2)	29(1)
C(9B)	7139(2)	5642(1)	-1335(2)	25(1)
C(10B)	7953(2)	4959(1)	130(2)	26(1)
C(11B)	6272(2)	4772(1)	1955(2)	25(1)
C(12B)	6293(3)	4334(1)	2986(2)	32(1)
C(13B)	7443(3)	3953(1)	2469(2)	32(1)
C(14B)	8628(2)	4268(1)	1780(2)	25(1)
C(15B)	10175(2)	4373(1)	2686(2)	25(1)
C(16B)	11216(3)	4723(1)	1943(2)	35(1)
C(17B)	9912(3)	4610(1)	4072(2)	30(1)
C(18B)	11013(3)	3863(1)	2910(2)	34(1)
C(19B)	6143(2)	5280(1)	2673(2)	24(1)
C(20B)	4380(3)	5795(1)	3740(2)	28(1)
C(21B)	3462(2)	5651(1)	4858(2)	25(1)

Table 3.4. Bond lengths [Å] and angles [°] for LWL01 (CCDC 258350).

O(1A)-N(1A)	1.2222(19)	C(15A)-C(16A)	1.517(3)
O(2A)-N(1A)	1.2370(18)	C(15A)-C(17A)	1.528(3)
O(3A)-C(3A)	1.359(2)	C(15A)-C(18A)	1.529(3)
O(3A)-C(7A)	1.432(2)	C(16A)-H(16A)	0.981(19)
O(4A)-C(4A)	1.3439(19)	C(16A)-H(16B)	0.98(2)
O(4A)-C(8A)	1.436(2)	C(16A)-H(16C)	1.07(2)
O(5A)-C(10A)	1.362(2)	C(17A)-H(17A)	1.004(19)
O(5A)-C(9A)	1.452(2)	C(17A)-H(17B)	0.99(2)
O(6A)-C(10A)	1.204(2)	C(17A)-H(17C)	1.05(2)
O(7A)-C(19A)	1.195(2)	C(18A)-H(18A)	0.94(2)
O(8A)-C(19A)	1.353(2)	C(18A)-H(18B)	0.98(2)
O(8A)-C(20A)	1.438(2)	C(18A)-H(18C)	0.99(2)
N(1A)-C(1A)	1.456(2)	C(20A)-C(21A)	1.471(3)
N(2A)-C(10A)	1.353(2)	C(20A)-H(20A)	0.99(2)
N(2A)-C(11A)	1.466(2)	C(20A)-H(20B)	0.97(2)
N(2A)-C(14A)	1.486(2)	O(1B)-N(1B)	1.222(2)
N(3A)-C(21A)	1.128(2)	O(2B)-N(1B)	1.216(2)
C(1A)-C(6A)	1.397(2)	O(3B)-C(3B)	1.364(2)
C(1A)-C(2A)	1.400(2)	O(3B)-C(7B)	1.435(2)
C(2A)-C(3A)	1.376(3)	O(4B)-C(4B)	1.360(2)
C(2A)-H(2A)	0.924(17)	O(4B)-C(8B)	1.432(2)
C(3A)-C(4A)	1.412(2)	O(5B)-C(10B)	1.357(2)
C(4A)-C(5A)	1.380(2)	O(5B)-C(9B)	1.442(2)
C(5A)-C(6A)	1.390(2)	O(6B)-C(10B)	1.209(2)
C(5A)-H(5A)	0.933(18)	O(7B)-C(19B)	1.193(2)
C(6A)-C(9A)	1.519(3)	O(8B)-C(19B)	1.349(2)
C(7A)-H(7A)	1.01(2)	O(8B)-C(20B)	1.448(2)
C(7A)-H(7B)	0.96(2)	N(1B)-C(1B)	1.458(2)
C(7A)-H(7C)	1.010(19)	N(2B)-C(10B)	1.352(2)
C(8A)-H(8A)	1.04(2)	N(2B)-C(11B)	1.461(2)
C(8A)-H(8B)	1.03(2)	N(2B)-C(14B)	1.479(2)
C(8A)-H(8C)	1.012(18)	N(3B)-C(21B)	1.137(2)
C(9A)-H(9A)	1.023(17)	C(1B)-C(6B)	1.389(3)
C(9A)-H(9B)	0.955(16)	C(1B)-C(2B)	1.403(3)
C(11A)-C(19A)	1.514(3)	C(2B)-C(3B)	1.360(2)
C(11A)-C(12A)	1.542(3)	C(2B)-H(2B)	0.923(15)
C(11A)-H(11A)	0.961(15)	C(3B)-C(4B)	1.410(2)
C(12A)-C(13A)	1.521(3)	C(4B)-C(5B)	1.379(2)
C(12A)-H(12A)	1.006(17)	C(5B)-C(6B)	1.397(2)
C(12A)-H(12B)	0.972(18)	C(5B)-H(5B)	0.983(15)
C(13A)-C(14A)	1.532(3)	C(6B)-C(9B)	1.515(3)
C(13A)-H(13A)	1.003(18)	C(7B)-H(7D)	1.042(19)
C(13A)-H(13B)	1.008(19)	C(7B)-H(7E)	0.945(19)
C(14A)-C(15A)	1.547(3)	C(7B)-H(7F)	1.012(19)
C(14A)-H(14A)	1.007(15)	C(8B)-H(8D)	0.976(18)

C(8B)-H(8E)	1.043(19)	C(1A)-C(2A)-H(2A)	116.1(10)
C(8B)-H(8F)	0.969(19)	O(3A)-C(3A)-C(2A)	125.56(17)
C(9B)-H(9C)	0.903(17)	O(3A)-C(3A)-C(4A)	115.44(15)
C(9B)-H(9D)	0.998(17)	C(2A)-C(3A)-C(4A)	119.00(17)
C(11B)-C(19B)	1.523(3)	O(4A)-C(4A)-C(5A)	125.16(16)
C(11B)-C(12B)	1.529(3)	O(4A)-C(4A)-C(3A)	114.87(15)
C(11B)-H(11B)	0.998(16)	C(5A)-C(4A)-C(3A)	119.97(16)
C(12B)-C(13B)	1.536(3)	C(4A)-C(5A)-C(6A)	122.62(17)
C(12B)-H(12C)	1.003(19)	C(4A)-C(5A)-H(5A)	120.1(11)
C(12B)-H(12D)	1.00(2)	C(6A)-C(5A)-H(5A)	117.2(11)
C(13B)-C(14B)	1.528(3)	C(5A)-C(6A)-C(1A)	116.11(16)
C(13B)-H(13C)	0.955(19)	C(5A)-C(6A)-C(9A)	118.85(15)
C(13B)-H(13D)	0.974(19)	C(1A)-C(6A)-C(9A)	125.02(15)
C(14B)-C(15B)	1.546(2)	O(3A)-C(7A)-H(7A)	107.0(11)
C(14B)-H(14B)	0.969(15)	O(3A)-C(7A)-H(7B)	112.0(12)
C(15B)-C(16B)	1.524(3)	H(7A)-C(7A)-H(7B)	112.5(16)
C(15B)-C(17B)	1.525(3)	O(3A)-C(7A)-H(7C)	113.2(10)
C(15B)-C(18B)	1.534(3)	H(7A)-C(7A)-H(7C)	108.5(14)
C(16B)-H(16D)	0.99(2)	H(7B)-C(7A)-H(7C)	103.8(15)
C(16B)-H(16E)	1.03(2)	O(4A)-C(8A)-H(8A)	106.2(10)
C(16B)-H(16F)	0.97(2)	O(4A)-C(8A)-H(8B)	111.7(11)
C(17B)-H(17D)	1.034(19)	H(8A)-C(8A)-H(8B)	105.6(15)
C(17B)-H(17E)	0.972(19)	O(4A)-C(8A)-H(8C)	110.1(10)
C(17B)-H(17F)	0.99(2)	H(8A)-C(8A)-H(8C)	113.5(15)
C(18B)-H(18D)	1.02(2)	H(8B)-C(8A)-H(8C)	109.7(15)
C(18B)-H(18E)	1.01(2)	O(5A)-C(9A)-C(6A)	110.80(14)
C(18B)-H(18F)	0.929(18)	O(5A)-C(9A)-H(9A)	105.5(9)
C(20B)-C(21B)	1.463(3)	C(6A)-C(9A)-H(9A)	111.7(9)
C(20B)-H(20C)	1.009(17)	O(5A)-C(9A)-H(9B)	108.7(9)
C(20B)-H(20D)	0.929(18)	C(6A)-C(9A)-H(9B)	110.3(10)
		H(9A)-C(9A)-H(9B)	109.7(13)
C(3A)-O(3A)-C(7A)	117.47(14)	O(6A)-C(10A)-N(2A)	124.79(17)
C(4A)-O(4A)-C(8A)	117.07(14)	O(6A)-C(10A)-O(5A)	123.02(17)
C(10A)-O(5A)-C(9A)	113.15(14)	N(2A)-C(10A)-O(5A)	112.18(16)
C(19A)-O(8A)-C(20A)	115.89(14)	N(2A)-C(11A)-C(19A)	113.30(15)
O(1A)-N(1A)-O(2A)	121.68(15)	N(2A)-C(11A)-C(12A)	104.27(15)
O(1A)-N(1A)-C(1A)	119.54(15)	C(19A)-C(11A)-C(12A)	109.55(14)
O(2A)-N(1A)-C(1A)	118.76(15)	N(2A)-C(11A)-H(11A)	110.3(9)
C(10A)-N(2A)-C(11A)	123.26(15)	C(19A)-C(11A)-H(11A)	105.2(9)
C(10A)-N(2A)-C(14A)	118.35(14)	C(12A)-C(11A)-H(11A)	114.5(9)
C(11A)-N(2A)-C(14A)	113.13(14)	C(13A)-C(12A)-C(11A)	104.85(15)
C(6A)-C(1A)-C(2A)	122.79(16)	C(13A)-C(12A)-H(12A)	112.4(10)
C(6A)-C(1A)-N(1A)	121.31(15)	C(11A)-C(12A)-H(12A)	108.2(10)
C(2A)-C(1A)-N(1A)	115.89(16)	C(13A)-C(12A)-H(12B)	114.1(10)
C(3A)-C(2A)-C(1A)	119.51(18)	C(11A)-C(12A)-H(12B)	112.2(10)
C(3A)-C(2A)-H(2A)	124.4(10)	H(12A)-C(12A)-H(12B)	105.0(13)

C(12A)-C(13A)-C(14A)	105.86(16)	C(3B)-O(3B)-C(7B)	116.86(14)
C(12A)-C(13A)-H(13A)	111.7(10)	C(4B)-O(4B)-C(8B)	118.23(14)
C(14A)-C(13A)-H(13A)	112.0(10)	C(10B)-O(5B)-C(9B)	114.93(15)
C(12A)-C(13A)-H(13B)	108.9(11)	C(19B)-O(8B)-C(20B)	115.40(14)
C(14A)-C(13A)-H(13B)	108.2(11)	O(2B)-N(1B)-O(1B)	122.31(16)
H(13A)-C(13A)-H(13B)	110.0(14)	O(2B)-N(1B)-C(1B)	118.76(17)
N(2A)-C(14A)-C(13A)	102.60(15)	O(1B)-N(1B)-C(1B)	118.91(17)
N(2A)-C(14A)-C(15A)	113.98(15)	C(10B)-N(2B)-C(11B)	121.96(15)
C(13A)-C(14A)-C(15A)	116.00(15)	C(10B)-N(2B)-C(14B)	120.59(15)
N(2A)-C(14A)-H(14A)	105.7(8)	C(11B)-N(2B)-C(14B)	113.22(15)
C(13A)-C(14A)-H(14A)	110.2(8)	C(6B)-C(1B)-C(2B)	122.72(16)
C(15A)-C(14A)-H(14A)	107.9(8)	C(6B)-C(1B)-N(1B)	121.46(17)
C(16A)-C(15A)-C(17A)	109.93(17)	C(2B)-C(1B)-N(1B)	115.79(17)
C(16A)-C(15A)-C(18A)	108.58(19)	C(3B)-C(2B)-C(1B)	119.78(18)
C(17A)-C(15A)-C(18A)	107.81(17)	C(3B)-C(2B)-H(2B)	118.8(10)
C(16A)-C(15A)-C(14A)	112.04(16)	C(1B)-C(2B)-H(2B)	121.4(10)
C(17A)-C(15A)-C(14A)	107.65(16)	C(2B)-C(3B)-O(3B)	125.75(17)
C(18A)-C(15A)-C(14A)	110.73(16)	C(2B)-C(3B)-C(4B)	119.09(17)
C(15A)-C(16A)-H(16A)	108.9(11)	O(3B)-C(3B)-C(4B)	115.17(14)
C(15A)-C(16A)-H(16B)	113.0(12)	O(4B)-C(4B)-C(5B)	124.76(16)
H(16A)-C(16A)-H(16B)	104.2(16)	O(4B)-C(4B)-C(3B)	114.99(15)
C(15A)-C(16A)-H(16C)	112.8(11)	C(5B)-C(4B)-C(3B)	120.25(15)
H(16A)-C(16A)-H(16C)	112.6(16)	C(4B)-C(5B)-C(6B)	121.93(18)
H(16B)-C(16A)-H(16C)	104.9(17)	C(4B)-C(5B)-H(5B)	119.8(9)
C(15A)-C(17A)-H(17A)	108.6(11)	C(6B)-C(5B)-H(5B)	118.2(9)
C(15A)-C(17A)-H(17B)	109.0(11)	C(1B)-C(6B)-C(5B)	116.22(17)
H(17A)-C(17A)-H(17B)	104.7(15)	C(1B)-C(6B)-C(9B)	123.96(15)
C(15A)-C(17A)-H(17C)	110.4(11)	C(5B)-C(6B)-C(9B)	119.82(16)
H(17A)-C(17A)-H(17C)	111.4(15)	O(3B)-C(7B)-H(7D)	104.1(10)
H(17B)-C(17A)-H(17C)	112.5(16)	O(3B)-C(7B)-H(7E)	108.4(11)
C(15A)-C(18A)-H(18A)	107.4(11)	H(7D)-C(7B)-H(7E)	113.1(15)
C(15A)-C(18A)-H(18B)	110.5(12)	O(3B)-C(7B)-H(7F)	111.9(10)
H(18A)-C(18A)-H(18B)	103.2(17)	H(7D)-C(7B)-H(7F)	111.7(14)
C(15A)-C(18A)-H(18C)	113.0(12)	H(7E)-C(7B)-H(7F)	107.7(14)
H(18A)-C(18A)-H(18C)	113.1(17)	O(4B)-C(8B)-H(8D)	105.0(10)
H(18B)-C(18A)-H(18C)	109.2(17)	O(4B)-C(8B)-H(8E)	110.2(9)
O(7A)-C(19A)-O(8A)	123.81(17)	H(8D)-C(8B)-H(8E)	108.9(14)
O(7A)-C(19A)-C(11A)	127.71(17)	O(4B)-C(8B)-H(8F)	106.3(10)
O(8A)-C(19A)-C(11A)	108.41(15)	H(8D)-C(8B)-H(8F)	114.3(14)
O(8A)-C(20A)-C(21A)	110.22(16)	H(8E)-C(8B)-H(8F)	111.8(14)
O(8A)-C(20A)-H(20A)	106.6(11)	O(5B)-C(9B)-C(6B)	111.39(15)
C(21A)-C(20A)-H(20A)	106.4(11)	O(5B)-C(9B)-H(9C)	104.7(11)
O(8A)-C(20A)-H(20B)	111.4(11)	C(6B)-C(9B)-H(9C)	111.7(11)
C(21A)-C(20A)-H(20B)	107.6(11)	O(5B)-C(9B)-H(9D)	107.2(9)
H(20A)-C(20A)-H(20B)	114.6(16)	C(6B)-C(9B)-H(9D)	111.8(9)
N(3A)-C(21A)-C(20A)	179.4(2)	H(9C)-C(9B)-H(9D)	109.8(14)

O(6B)-C(10B)-N(2B)	125.92(17)	C(15B)-C(18B)-H(18E)	109.0(12)
O(6B)-C(10B)-O(5B)	123.44(17)	H(18D)-C(18B)-H(18E)	114.3(15)
N(2B)-C(10B)-O(5B)	110.64(16)	C(15B)-C(18B)-H(18F)	111.3(11)
N(2B)-C(11B)-C(19B)	111.82(15)	H(18D)-C(18B)-H(18F)	103.6(15)
N(2B)-C(11B)-C(12B)	104.98(15)	H(18E)-C(18B)-H(18F)	110.6(15)
C(19B)-C(11B)-C(12B)	111.33(15)	O(7B)-C(19B)-O(8B)	124.56(18)
N(2B)-C(11B)-H(11B)	109.3(9)	O(7B)-C(19B)-C(11B)	126.50(17)
C(19B)-C(11B)-H(11B)	107.6(10)	O(8B)-C(19B)-C(11B)	108.82(15)
C(12B)-C(11B)-H(11B)	111.8(10)	O(8B)-C(20B)-C(21B)	107.46(16)
C(11B)-C(12B)-C(13B)	104.15(16)	O(8B)-C(20B)-H(20C)	108.8(9)
C(11B)-C(12B)-H(12C)	110.1(10)	C(21B)-C(20B)-H(20C)	108.8(9)
C(13B)-C(12B)-H(12C)	110.4(10)	O(8B)-C(20B)-H(20D)	107.2(10)
C(11B)-C(12B)-H(12D)	111.7(11)	C(21B)-C(20B)-H(20D)	109.5(11)
C(13B)-C(12B)-H(12D)	112.0(11)	H(20C)-C(20B)-H(20D)	114.8(15)
H(12C)-C(12B)-H(12D)	108.5(15)	N(3B)-C(21B)-C(20B)	178.6(2)
C(14B)-C(13B)-C(12B)	105.92(17)		
C(14B)-C(13B)-H(13C)	107.9(11)		
C(12B)-C(13B)-H(13C)	107.5(11)		
C(14B)-C(13B)-H(13D)	112.8(11)		
C(12B)-C(13B)-H(13D)	109.6(11)		
H(13C)-C(13B)-H(13D)	112.8(17)		
N(2B)-C(14B)-C(13B)	102.68(15)		
N(2B)-C(14B)-C(15B)	114.51(15)		
C(13B)-C(14B)-C(15B)	115.33(17)		
N(2B)-C(14B)-H(14B)	105.8(9)		
C(13B)-C(14B)-H(14B)	112.4(9)		
C(15B)-C(14B)-H(14B)	105.8(9)		
C(16B)-C(15B)-C(17B)	108.71(17)		
C(16B)-C(15B)-C(18B)	107.83(18)		
C(17B)-C(15B)-C(18B)	110.37(17)		
C(16B)-C(15B)-C(14B)	110.95(16)		
C(17B)-C(15B)-C(14B)	112.09(16)		
C(18B)-C(15B)-C(14B)	106.80(15)		
C(15B)-C(16B)-H(16D)	110.1(11)		
C(15B)-C(16B)-H(16E)	113.1(11)		
H(16D)-C(16B)-H(16E)	107.2(15)		
C(15B)-C(16B)-H(16F)	112.0(11)		
H(16D)-C(16B)-H(16F)	109.3(16)		
H(16E)-C(16B)-H(16F)	104.9(15)		
C(15B)-C(17B)-H(17D)	111.4(10)		
C(15B)-C(17B)-H(17E)	110.1(10)		
H(17D)-C(17B)-H(17E)	107.1(15)		
C(15B)-C(17B)-H(17F)	113.3(11)		
H(17D)-C(17B)-H(17F)	107.5(15)		
H(17E)-C(17B)-H(17F)	107.2(15)		
C(15B)-C(18B)-H(18D)	107.9(11)		

Table 3.5. Anisotropic displacement parameters ($\text{\AA}^2 \times 10^4$) for LWL01 (CCDC 258350). The anisotropic displacement factor exponent takes the form: $-2\pi^2 [h^2 a^{*2} U^{11} + \dots + 2 h k a^* b^* U^{12}]$

	U ¹¹	U ²²	U ³³	U ²³	U ¹³	U ¹²
O(1A)	671(11)	400(9)	223(7)	-19(7)	10(7)	268(8)
O(2A)	374(8)	300(8)	221(7)	28(6)	-71(6)	61(6)
O(3A)	333(8)	267(8)	224(7)	11(6)	32(6)	110(6)
O(4A)	356(8)	280(7)	204(7)	-7(6)	-5(6)	120(6)
O(5A)	244(7)	202(7)	212(6)	15(6)	-23(5)	25(6)
O(6A)	311(8)	430(9)	317(8)	113(7)	-128(6)	-114(7)
O(7A)	273(7)	236(7)	343(7)	-68(6)	-36(6)	63(6)
O(8A)	197(7)	241(7)	280(7)	-65(6)	-32(6)	1(6)
N(1A)	292(9)	254(9)	198(8)	8(7)	0(7)	14(8)
N(2A)	216(8)	205(8)	180(8)	18(7)	-43(6)	-3(7)
N(3A)	780(16)	392(11)	315(11)	-48(9)	46(10)	-129(11)
C(1A)	230(10)	207(10)	191(10)	4(8)	19(8)	-40(8)
C(2A)	214(10)	220(10)	201(10)	52(8)	-8(8)	-2(8)
C(3A)	204(10)	184(10)	259(10)	-6(8)	29(8)	-5(8)
C(4A)	220(10)	236(11)	170(10)	-15(8)	17(8)	-6(8)
C(5A)	199(10)	197(10)	195(10)	25(8)	-2(8)	25(8)
C(6A)	210(10)	217(10)	181(9)	7(8)	26(8)	-34(8)
C(7A)	305(13)	234(12)	304(12)	52(10)	34(10)	80(10)
C(8A)	413(14)	319(13)	202(11)	-18(9)	-9(10)	136(11)
C(9A)	276(11)	265(11)	166(10)	9(9)	-15(9)	11(9)
C(10A)	270(11)	241(11)	261(10)	-24(8)	13(9)	-1(9)
C(11A)	213(10)	217(10)	203(9)	-14(8)	7(8)	6(8)
C(12A)	213(11)	265(11)	257(11)	-13(9)	-36(8)	38(9)
C(13A)	276(11)	209(11)	245(11)	-22(9)	14(9)	28(9)
C(14A)	252(11)	218(11)	196(10)	-5(8)	-27(8)	-33(8)
C(15A)	207(10)	280(11)	253(10)	17(9)	30(8)	21(9)
C(16A)	314(13)	467(15)	302(12)	-67(11)	82(11)	27(12)
C(17A)	306(13)	363(13)	384(13)	52(11)	57(11)	-16(11)
C(18A)	291(13)	416(16)	488(16)	113(13)	83(12)	96(12)
C(19A)	238(10)	243(11)	162(9)	45(8)	17(8)	26(9)
C(20A)	267(12)	217(11)	275(11)	-16(9)	-46(9)	-14(9)
C(21A)	374(13)	206(11)	283(12)	-28(9)	-58(10)	-24(9)
O(1B)	439(9)	522(10)	287(8)	-43(7)	-98(7)	-86(8)
O(2B)	1186(17)	607(12)	236(9)	98(8)	-117(9)	-357(11)
O(3B)	305(8)	286(8)	227(7)	18(6)	18(6)	-78(6)
O(4B)	294(7)	282(7)	174(7)	0(6)	-6(5)	-71(6)
O(5B)	208(7)	267(7)	227(7)	-24(6)	-3(5)	21(6)
O(6B)	286(8)	421(9)	217(7)	-14(6)	47(6)	93(7)
O(7B)	227(8)	326(8)	313(7)	-86(6)	52(6)	-76(6)

O(8B)	209(7)	284(8)	369(8)	-116(6)	82(6)	-45(6)
N(1B)	396(10)	340(11)	222(9)	-26(8)	-20(8)	33(9)
N(2B)	213(9)	282(9)	208(8)	-43(7)	1(7)	17(7)
N(3B)	494(12)	287(10)	309(10)	0(8)	113(9)	-28(9)
C(1B)	254(10)	281(11)	191(10)	-36(8)	-13(8)	79(9)
C(2B)	291(11)	264(11)	199(10)	21(9)	58(8)	49(9)
C(3B)	215(10)	236(10)	217(10)	-34(8)	9(8)	0(9)
C(4B)	219(10)	255(11)	164(9)	-28(8)	9(8)	30(9)
C(5B)	192(10)	264(11)	209(10)	-9(9)	32(8)	14(9)
C(6B)	186(10)	258(11)	208(10)	-35(8)	14(8)	60(8)
C(7B)	340(13)	286(12)	214(11)	32(9)	28(10)	-25(10)
C(8B)	340(14)	355(14)	171(11)	15(9)	-51(10)	-71(10)
C(9B)	212(11)	306(12)	223(11)	-32(9)	-25(9)	41(9)
C(10B)	202(11)	339(12)	228(10)	-75(9)	-43(9)	15(9)
C(11B)	204(10)	301(11)	235(10)	-63(9)	15(8)	-19(9)
C(12B)	300(12)	329(13)	337(13)	-23(10)	78(10)	-60(10)
C(13B)	309(12)	267(12)	382(13)	-32(10)	-15(10)	-67(10)
C(14B)	239(11)	265(12)	225(10)	-70(8)	2(9)	4(9)
C(15B)	235(11)	245(10)	247(10)	-9(8)	-30(8)	-14(9)
C(16B)	220(12)	483(15)	320(13)	43(11)	-36(10)	-50(11)
C(17B)	318(13)	328(13)	237(11)	-16(9)	-25(10)	-27(10)
C(18B)	295(14)	374(14)	336(13)	-76(11)	-71(11)	32(11)
C(19B)	223(11)	317(12)	180(10)	6(8)	9(8)	-48(9)
C(20B)	267(12)	251(11)	318(12)	-33(9)	67(10)	2(9)
C(21B)	282(11)	200(11)	250(11)	-24(9)	11(9)	8(8)

Table 3.6. Hydrogen coordinates ($\times 10^4$) and isotropic displacement parameters ($\text{\AA}^2 \times 10^3$) for LWL01 (CCDC 258350).

	x	y	z	U_{iso}
H(2A)	6510(20)	1420(6)	12506(18)	17(5)
H(5A)	3400(20)	2392(7)	9379(18)	27(5)
H(7A)	7840(20)	488(7)	10182(19)	34(5)
H(7B)	6750(20)	602(8)	11430(20)	37(6)
H(7C)	8260(20)	915(7)	11385(18)	26(5)
H(8A)	3960(20)	1791(7)	6220(20)	40(6)
H(8B)	4190(20)	2314(8)	7138(19)	39(6)
H(8C)	2710(20)	1936(6)	7422(17)	21(5)
H(9A)	2310(20)	2641(6)	12384(17)	18(5)
H(9B)	3828(18)	2998(6)	12364(16)	12(4)
H(11A)	327(18)	3562(6)	9315(16)	9(4)
H(12A)	563(19)	3890(7)	6566(18)	21(5)
H(12B)	-480(20)	4150(6)	7589(16)	17(5)
H(13A)	2060(20)	4615(7)	7136(18)	27(5)
H(13B)	1560(20)	4609(7)	8730(20)	35(5)
H(14A)	3870(17)	4246(5)	9291(15)	7(4)
H(16A)	4460(20)	3697(7)	5421(18)	31(5)
H(16B)	2890(30)	3965(8)	5580(20)	48(6)
H(16C)	3070(20)	3400(8)	6250(20)	46(6)
H(17A)	6070(20)	4410(7)	6478(18)	29(5)
H(17B)	5760(20)	4619(7)	7950(20)	42(6)
H(17C)	4380(20)	4727(8)	6600(20)	43(6)
H(18A)	6430(20)	3567(7)	7320(19)	31(5)
H(18B)	5330(20)	3278(9)	8140(20)	42(6)
H(18C)	6280(20)	3740(8)	8890(20)	42(6)
H(20A)	-2760(20)	2662(7)	6498(19)	33(5)
H(20B)	-1170(20)	2332(8)	6937(19)	35(6)
H(2B)	10007(17)	7060(6)	-2117(16)	7(4)
H(5B)	8530(17)	5902(6)	1130(16)	10(4)
H(7D)	12410(20)	7880(7)	58(18)	30(5)
H(7E)	10760(20)	7785(7)	-945(18)	26(5)
H(7F)	12240(20)	7490(7)	-1341(19)	24(5)
H(8D)	10850(20)	6350(6)	4038(18)	18(4)
H(8E)	10560(20)	5874(7)	2953(17)	26(5)
H(8F)	9110(20)	6264(6)	3237(17)	23(5)
H(9C)	6180(20)	5753(6)	-1655(17)	15(5)
H(9D)	7545(18)	5414(6)	-2032(17)	18(5)
H(11B)	5380(19)	4745(6)	1218(17)	22(5)
H(12C)	6680(20)	4455(7)	3940(20)	29(5)
H(12D)	5240(20)	4184(7)	3012(19)	42(6)

H(13C)	6880(20)	3751(7)	1770(19)	31(5)
H(13D)	7920(20)	3753(7)	3240(20)	35(6)
H(14B)	8915(17)	4112(5)	941(16)	4(4)
H(16D)	10680(20)	5049(8)	1727(19)	36(6)
H(16E)	11510(20)	4575(7)	1030(20)	39(6)
H(16F)	12200(20)	4785(7)	2487(19)	39(6)
H(17D)	9330(20)	4951(8)	3939(18)	34(5)
H(17E)	10900(20)	4679(6)	4607(18)	24(5)
H(17F)	9310(20)	4391(8)	4650(20)	37(6)
H(18D)	11070(20)	3702(7)	1960(20)	39(6)
H(18E)	10460(20)	3653(8)	3560(20)	43(6)
H(18F)	12050(20)	3907(6)	3250(17)	20(5)
H(20C)	5410(20)	5937(6)	4158(16)	16(4)
H(20D)	3800(20)	6012(7)	3133(17)	21(5)

3.6.2 *Electrophysiology and molecular biology general:*

Unless otherwise stated, chemicals and molecular biology reagents were purchased from commercial sources and used as is. *Xenopus laevis* were purchased from Xenopus Express (Plant City, FL) and Xenopus One (Dexter, MI).

3.6.2.1 *Site-directed mutagenesis of subunits of nAChR*

Mutagenetic primers were custom ordered from Integrated DNA Technology (IDT) Inc. (San Diego, CA) in 25 nmole amounts with standard desalting. These primers had the following properties: length: 25-45 bases, $T_m \geq 78$ °C, CG content 40%-50 %, and terminates with one or more C/G at the 3' end. Quickchange kits from Qiagen (Valencia, CA) were used.

To a PCR tube was added 10 x polymerase buffer (5 μ L), 5-50 ng of circular DNA (2 μ L volume), 125 ng of mutagenic primer #1 (125 μ L), 125 ng of mutagenic primer #2 (125 μ L), 25 mM dNTP mix (1 μ L) and RNase free water (38.5 μ L) for total volume of 49 μ L. The reaction was mixed by gentle pipetting. Polymerase (1 μ L) was added to the reaction mixture and it was mixed. The reaction mixture was subject to the following cycling parameters:

Cycle 1 (1 cycle): 95 °C for 30 s.

Cycle 2 (18 cycles): Step 1 – 95 °C for 30 s.

Step 2 – 55 to 61 °C for 1 min.

Step 3 – 68 °C for 10 min.

Cycle 3 (1 cycle): 68 °C for 7 min.

Hold at 4 °C until digestion with Dpn I.

The Quickchange reactions were screened by electrophoresis through 1 % agarose gel. 10 μ L of each Quickchange reaction mixture was removed and mixed with 2 μ L 6 x DNA gel-loading buffer (0.25 % bromophenol blue, 0.25 % xylene cyanol FF, 30 % glycerol in Millipore water) and resolved on a 1 % agarose gel for 1 hr, followed by visualization with ethidium bromide. 1 μ L of Dpn I was then added to each reaction and the reaction was incubated at 37 °C for 1 h. Only reactions that showed amplification were transformed into Top10 cells.

3.6.2.2 Transformation of Quickchange reactions

1 μ L of a Quickchange reaction was added to 40 μ L of Blue Top10 cells that had been thawed on ice. The cells were mixed by gentle pipetting. The mixture was electroporated at 1800 V using a chilled 0.1 mm cuvette. 500 μ L of SOC media at 37 °C was added mixed with the cells. The mixture was removed and placed in a 5 mL Falcon tube. The recovered bacteria were incubated at 37 °C with shaking (300 rpm) for 20 min. Each culture was then plated on LB-agar supplemented with ampicillin. The plates were incubated upside down at 37 °C for 10-12 h. Distinct colonies were picked and used to inoculate cultures for minipreps. The miniprep DNA was sequenced to select for the correct mutant.

The primers used to make the mutations were (mutation site shown in red):

Alpha subunit nAChR:

Pro272TAG

5'-CCACCTCCAGCGCTGTG**TAG**CTGATCGGGAAGTATATG-3'

Pro272TAG Reverse complement

5'-CATATACTTCCCGATCAGCTACACAGCGCTGGAGGTGG-3'

Pro272Ala

5'-CCACCTCCAGCGCTGTGGCCCTGATCGGGAAGTATATG-3'

Pro272Ala reverse complement

5'-CATATACTTCCCGATCAGGGCCACAGCGCTGGAGGTGG-3'

Pro272Gly

5'-CCACCTCCAGCGCTGTGGCCCTGATCGGGAAGTATATG-3'

Pro272Gly reverse complement

5'-CATATACTTCCCGATCAGGCCACAGCGCTGGAGGTGG-3'

Pro272Val

5'-CCACCTCCAGCGCTGTGGTCCTGATCGGGAAGTATATG-3'

Pro272Val reverse complement

5'-CATATACTTCCCGATCAGGACCACAGCGCTGGAGGTGG-3'

Pro265TAG

5'-GGTCATTGTGGAGCTAATCTAGTCCACCTCCAGCGC-3'

Pro265TAG reverse complement

5'-GCGCTGGAGGTGGACTAGATTAGCTCCACAATGACC-3'

Pro265Val

5'-GGTCATTGTGGAGCTAATCGTTCCACCTCCAGCGC-3'

Pro265Val reverse Complement

5'-GCGCTGGAGGTGGAAACGATTAGCTCCACAATGACC-3'

Pro265Gly

5'-GGTCATTGTGGAGCTAATCGGTTCCACCTCCAGCGC-3'

Pro265Gly reverse complement

5'-GCGCTGGAGGTGGAACCGATTAGCTCCACAATGACC-3'

*Pro265Ala*5'-GGTCATTGTGGAGCTAATC**GCT**TCCACCTCCAGCGC-3'*Pro265Ala reverse Complement*

5'-GCGCTGGAGGTGGAAGCGATTAGCTCCACAATGACC-3'

3.6.2.3 mRNA Transcription from plasmid DNA

Plasmid DNA linearization: Plasmid DNA (5-10 µg, 30 µL) containing the desired subunit gene was mixed with 10 x Buffer (5 µL) and DEPC/nuclease free water (12 µL). To the mixture was added the appropriate restriction enzyme (3 µL). The reaction mixture was mixed by pipetting and incubated at 37 °C for 6 hours to overnight. A sample of the reaction mixture was then resolved on a 1 % agarose gel with ethidium bromide staining to ensure the plasmid DNA was completely linearized. If the plasmid DNA was not completely linearized, additional restriction enzyme (3 µL) was added, the reaction was incubated at 37 °C for another 4 hours, and followed by agarose gel analysis. Once the plasmid DNA was completely linearized, the reaction was heat inactivated for 20 min. at 65 °C.

Work up for Plasmid DNA linearization (follows Qiagen MinElute PCR Purification Kit protocol): Ethanol (96%–100 %) was added to Buffer PE before use (see bottle label for volume). All centrifugation steps were at 14,000 rpm in a tabletop micro-centrifuge. Five volumes of Buffer PB were added to 1 volume of linearization reaction and mixed by pipetting. A MinElute column was placed in a provided 2 mL collection tube. The reaction mix was applied to the MinElute column and centrifuged for 1 min. The flow-through was

discarded and the MinElute was placed back in the same 2 mL collection tube. The DNA was washed by an application of Buffer PE (750 μ L) and centrifuged for 1 min. The flow-through was discarded and the MinELute was placed in the same collection tube. The column was centrifuged for an additional 1 min. to ensure all residual ethanol was removed from the column. The MinElute column was placed in a 1.5 mL collection tube. The DNA was eluted from the column by adding DEPC/nuclease free water (9 μ L) directly to the center of the column membrane, incubating for 1 min. and then centrifuging for 1min. 8 μ L was recovered, which was used directly in mRNA transcription reactions.

T7 mMessage Machine Transcription (Uses Ambion T7 mMessage Transcription Kit): 10x transcription buffer (2 μ L), 2 x NTPs (10 μ L), linearized plasmid DNA (4 μ L), DEPC/nuclease free water (2 μ L) were combined and mixed by pipetting. To the mixture was added T7 mMessage Machine Enzyme Mix (2 μ L). Subsequently, the reaction was mixed by pipetting and incubated for 2 hours at 37 °C. The reaction was quenched by the addition of 1 μ L of DNase I, followed by incubating at 37 °C for 15 min.

mRNA Cleanup (uses Qiagen RNeasy Mini for RNA Cleanup Kit): 10 μ L of β -ME was added per 1 mL Buffer RLT. For first time use, 4 volumes of ethanol (96%–100 %) was added to Buffer RPE (supplied as a concentrate), as indicated on the bottle, to obtain a working solution. The volume of the T7mMessage Machine Transcription reaction was adjusted to 100 μ L with DEPC/nuclease free water. Buffer RLT (350 μ L) was added and the reaction was mixed thoroughly by pipetting. To the diluted RNA, was added ethanol (96%–100 %, 250 μ L). The mixture was mixed thoroughly and applied to an RNeasy mini column placed in a 2 ml collection tube. The tube was closed gently and centrifuged for 15 sec. The flow-through and collection tube were discarded. The column was placed in a new 2 mL

collection tube. Buffer RPE (500 μ L) was pipetted into the column and the column was centrifuged for 15 sec. Another portion of Buffer RPE (500 μ L) was added to the column and the column was centrifuged for 2 min. to ensure the RNeasy silica-gel membrane is completely dry. The flow-through and collection tube were discarded and the column was placed in a new 2 mL collection tube and centrifuged for 1 min. to remove all residual ethanol. The RNA was eluted from the column by transferring the RNeasy column to a new 1.5 ml collection tube. DEPC/nuclease free water (30–50 μ L) was pipetted directly onto the RNeasy silica-gel membrane. The tube was closed and centrifuged for 1 min. to elute. The eluted solution was reapplied to the column and centrifuged for 1 min. to increase yield.

3.6.2.4 *tRNA transcription from plasmid DNA*

Plasmid DNA linearization: Plasmid DNA (50-60 μ g, 180 μ L) was mixed with Buffer 4 (60 μ L) and DEPC/nuclease free water (342 μ L). To the mixture was added the Fok I (18 μ L). The reaction mixture was mixed by pipetting and incubated at 37 °C for 6 hours to overnight. A sample of the reaction mixture was then resolved on a 1 % agarose gel to ensure the plasmid DNA was completely linearized. If the plasmid DNA was not completely linearized, additional Fok I (6 μ L) was added, the reaction was incubated at 37 °C for another 4 hours, and followed by agarose gel analysis. Once the plasmid DNA was completely linearized, the reaction was heat inactivated for 20 min. at 65 °C.

Linearization workup: All centrifugation steps are at 14,000 rpm. The reaction was split into 2 tubes. To each tube, PCI (300 μ L) was added and mixture was vortexed for 1 min. followed by centrifugation for 2 min. The aqueous layer (top layer) was removed and saved. To the organic layer was added DEPC/nuclease free water (150 μ L), which was then

vortexed for 1 min. and centrifuged for 2 min. The aqueous layer (top layer) was removed and saved. The saved aqueous layers were combined and vortexed briefly. CI (450 μ L) was added to the combined aqueous layers and mixture was vortexed for 1 min., followed by centrifugation for 2 min. The aqueous layer (top layer) was removed. To the organic layer was added DEPC/nuclease free water (150 μ L), which was then vortexed for 1 min. and centrifuged for 2 min. The aqueous layer (top layer) was removed and split into 2 tubes (300 μ L each). To each tube was added: 1 μ L seedDNA, 30 μ L 5M NH_4OAc , and 900 μ L EtOH. The tubes were stored at $-20\text{ }^\circ\text{C}$ for at least an hour (usually overnight) to precipitate. The tubes were centrifuged at $4\text{ }^\circ\text{C}$ for 15 min. and the supernatant was removed. The pellets were dried under vacuum in a desiccator. All four pellets were redissolved in DEPC/nuclease free water (60 μ L total). The linearized DNA was used directly in the transcription.

T7 MEGAshortscript transcription (uses Ambion T7 MEGAshortscript Transcription Kit): 10x transcription buffer (12 μ L), 75 mM ATP (12 μ L), 75 mM CTP (12 μ L), 75 mM GTP (12 μ L), 75 mM UTP (12 μ L), linearized plasmid DNA (30 μ L), DEPC/nuclease free water (18 μ L) were combined and mixed by pipetting. To the mixture was added T7 MEGAshortscript Enzyme Mix (12 μ L). Subsequently, the reaction was mixed by pipetting and incubated for 2 hours at $37\text{ }^\circ\text{C}$. The DNA was digested by the addition of 6 μ L of DNase I, followed by incubating at $37\text{ }^\circ\text{C}$ for 15 min. The transcription reaction was quenched by the addition of DEPC/nuclease free water (414 μ L) and NH_4OAc "Stopping Solution" (60 μ L).

tRNA MEGAshortscript Transcription Workup: PCI (600 μ L) was added to the quenched reaction. The mixture was vortexed for 1 min then centrifuged for 2 min. The

aqueous layer (top layer) was removed and saved. To the organic layer was added DEPC/nuclease free water (300 μ L). It was then vortexed, centrifuged for 2 min. and the aqueous layer removed and saved. The aqueous layers were combined, vortexed briefly and then divided into two 450 μ L portions. A CI extraction was performed on each tube by adding CI (450 μ L), vortexing for 1 min, centrifuging for 2 min and then removing the aqueous layer (top layer). Isopropanol (450 μ L) was added to each aqueous extract. The mixture was stored at -20 $^{\circ}$ C overnight to precipitate. The tubes are centrifuged for 15 min. at 4 $^{\circ}$ C and the supernatant was removed. The pellets were dried under vacuum in a dessicator and then both pellets were dissolved and combined in DEPC/nuclease free water (100 μ L total).

Column purification of tRNA: 2 BD Bioscience CHROMA SPIN-30 DEPC-H₂O columns were equilibrated by spinning for 5 min. at 3000 rpm. (2 columns used to avoid overloading.) The flow-through was discarded and the columns were placed in new eppendorf tubes. The process was repeated until there was no more flow-through. The tRNA solution was divided in half (50 μ L each portions) and each portion was applied to one equilibrated column. Each portion was applied carefully to avoid touching the sides of the tube. The tRNA solution was eluted from the CHROMA SPIN-30 columns by centrifuging for 5 min. at 3000 rpm. The eluted tRNA solution from both columns was combined, yielding 100 μ L.

3.6.2.5 *tRNA ligation to dCA-unnatural amino acid*

Denature tRNA: 74-mer tRNA (30 µg) is brought to a volume of 45 µL using 10 mM HEPES, pH 7.5 (room temperature). It is placed in a beaker of boiling water and allowed to cool to 37 °C in air or in an ice bath.

2.5 x reaction mix: The following reagents were combined and mixed thoroughly to make the 2.5 x reaction mix used in ligations: 400 mM HEPES, pH 7.5 (25 µL), 100 mM DTT (10 µL), 200 mM MgCl₂ (25 µL), 10 mM ATP (thaw on ice, 4 µL), 5 mg/mL Ac-BSA (thaw on ice, 10 µL), DEPC/nuclease free water (25 µL), and RNase Inhibitor (1 µL).

Ligation reaction: The following were combined: DEPC/nuclease free water (7.8 µL), 2.5 x Reaction mix (room temp, 48 µL), dCA-aa (3mM in DMSO, 12 µL), tRNA/HEPES mix (45 µL), and T4 RNA ligase (7.2 µL). The reaction was vortexed and incubated at 37 °C for 30 min. The reaction is quenched with the addition of 3.0 M NaOAc, pH 5.0 (12.5 µL) and DEPC water (17.5 µL).

tRNA Ligation Workup: PCI, pH 5.2 (150 µL) was added to the quenched reaction. The mixture was vortexed for 1 min then centrifuged for 2 min. The aqueous layer (top layer) was removed and saved. To the organic layer was added 3 M NaOAc (6.3 µL) and DEPC/nuclease free water (68.7 µL). It was then vortexed, centrifuged for 2 min. and the aqueous layer removed and saved. The aqueous layers were combined. A CI extraction was performed on each tube by adding CI (225 µL), vortexing for 1 min., centrifuging for 2 min. and then removing the aqueous layer (top layer). Ethanol (200 proof, 675 µL) was added to the aqueous extract. The mixture was stored at -20 °C overnight to precipitate. The tube was centrifuged for 15 min. at 4 °C and the supernatant was removed. The pellet was dried under vacuum in a dessicator and then redissolved in 1 mM NaOAc, pH 4.5 (room temp, 25 µL).

Column purification of tRNA ligation: A BD Bioscience CHROMA SPIN-30 DEPC-H₂O column was equilibrated by spinning for 5 min. at 3000 rpm. The flow-through was discarded and the column was placed in new eppendorf tubes. The process was repeated until there was no more flow-through. The tRNA ligation solution was applied carefully to avoid touching the sides of the tube. The tRNA ligation solution was eluted from the CHROMA SPIN-30 column by centrifuging for 5 min. at 3000 rpm. 25 μ L was typically recovered.

MALDI Mass Spectrometry Analysis of tRNA Ligation: 3-HPA mix is made by combining 3-hydroxypicolinic acid (42 mg), picolinic acid (2 mg), and diammonium citrate (2 mg) in 9:1 water:CH₃CN (500 μ L). This solution was stored at -20 °C and was thawed and sonicated for 2 min. before each use. For the cation exchange treatment, a 20-200 μ L pipetman tip was cut at the bevel near the tip's end. The cut tip was used to place NH₄⁺-loaded cation exchange bead slurry (5 μ L) in an eppendorf. Using an uncut pipetman tip, the water was removed from the slurry, leaving the beads behind. Amino acid-tRNA solution (0.5 μ L) was applied to the beads. To the amino acid-tRNA bead mixture was added 3-HPA mix (2.5 μ L), followed by picofuging to get all the material at the bottom of the tube. The mixture was incubated at room temperature for 10 min. BSA calibration mix was made by combining α -CN matrix solution (2.2 μ L, saturated α -cyanohydroxycinnamic acid in 2:1 water/CH₃CN) with PE Biosystems BSA calibrant (0.2 μ L). The calibration mixture and tRNA matrix solution (0.5 μ L) were each spotted on separate areas on the MALDI plate and allowed to dry completely. The plate was loaded with Plate ID: Plate #1. The system was allowed to pump down to $\sim 3.0 \times 10^{-7}$ torr. The Voyager Instrument Control Panel was set to the following:

Mode/Digitizer:

Instrument mode: Operation Mode: Linear, Extraction type: Delayed, Polarity type: Positive,

Laser type: Internal, Laser rate type: Optimized

Linear Digitizer: Bin size: 0.5 ns, Vertical scale: 100 mV, Vertical offset: 0.0%, Input bandwidth: Full

Control Mode: Manual

Voltages: Voltage: 25,000 V, Grid voltage: 92.5 %, Guide wire: 0.15 %, Delay: 500 ns,

Spectrum acquisition: 100 Shots/spectrum, Mass range: 20,000-35,000 Da; Low mass gate: 10,000 Da

For the BSA Calibration, the Laser power was set to 2000. The Calibration was set to α -CN default. The BSA calibration spot was blasted with 100 shot scans. Typically ten 100 shot scans were accumulated and averaged. The file was saved and then file was opened in Data Explorer. Manual Calibration was performed on +2 and +3 BSA peaks (+2: 33,216 Da; +3: 22,144 Da). (Selected peaks by right-clicking around them). Match peaks, Plot, Apply calibration and Export calibration file. Returning to Instrument Control, the newly generated calibration file was loaded as External File.

For the amino acid-tRNA samples, the Laser Power was set to 2500. The spots were blasted with 100 scan shot. Typically ten 100 shot scans were accumulated and averaged. The average scan was saved. To work up the data in Data Explorer, the mass range was set to 22,000-27,000. The Noise Filter was set to 1.0 and Gaussian Smoothing was set to 11 pts. Unligated 74-mer has a mass of 23,700 and hydrolyzed ligation product (76-mer) has a mass of 24,300.

3.6.2.6 *Injection of Stage VI Xenopus laevis oocytes*

Stage VI oocytes of *Xenopus laevis* were harvested according to approved protocol (Qi Huang and Purnima Deshpande, *Lester Laboratory*, California Institute of Technology, Pasadena, CA). Charged tRNA was deprotected immediately prior to injection into oocytes. Deprotection was performed by photolysis for 5 min. using an Arc Lamp (Oriol Corporation, Stratford, CT), powered to 400 W and filtered for 350 nm light. Typically, 25 ng of deprotected charged tRNA was injected along with 15 ng of mRNA in a total volume of 50 nL per oocyte. mRNA was prepared as previously described. Ligation of dCA coupled unnatural amino acid to 74-mer tRNA was performed as previously described.

Oocytes were injected using glass injection needles pulled from 10 μ L sp1 8 inch Borosilicate capillaries (Item #3-000-210-G8, Drummond Scientific, Broomall, PA). Injection needles were pulled on a KOPF Vertical Pipette Puller set on 13.3 (David Kopf Instruments, Tujunga, CA). The tip of the injection needle was broken off using tweezers to a diameter of \sim 25 μ m as visualized under a microscope (*under setting 2.0, one tick mark on eyepiece ruler equals 50 μ m*, Model S6E, Leica Microsystems, Wetzlar, Germany). The needle was filled with mineral oil and put on a 10 μ L microdispenser (Drummond Digital Microdispenser, Drummond Scientific Co., Broomall, PA). The deprotected amino acid-tRNA with mRNA mixture was drawn into the injection needle and then used to inject each oocyte with 50 nL of the mixture. Oocytes were then incubated at 18 $^{\circ}$ C in ND96 with 5 % horse serum.

3.6.2.7 *Two-electrode voltage clamp electrophysiological analysis*

Recordings were made 36-72 h post-injection in two-electrode voltage cell clamp mode using an OpusXpress (Axon Instruments, now part of Molecular Devices, Novato, CA). Oocytes were perfused with Ca^{+2} free ND96.

3.6.2.8 20 x Ca^{+2} free ND96

Mix together NaCl (56.10 g), KCl (1.49 g), $\text{MgCl}_2 \cdot 6\text{H}_2\text{O}$ (2.03 g), and HEPES (11.92 g) in millipore water (~400 mL). Adjust the mixture to pH = 7.5 with NaOH. Add water to make a total volume of 500 mL. Filter through a 0.2 μm filter (Nalgene). Store at 4 °C. Dilute with Millipore water to make 1x Ca^{+2} free ND96. The osmolarity of the 1x Ca^{+2} free ND96 was checked to ensure that it is between 195 and 240.

3.6.2.9 20 x ND96

Mix together NaCl (56.10 g), KCl (1.49 g), $\text{MgCl}_2 \cdot 6\text{H}_2\text{O}$ (2.03 g), $\text{CaCl}_2 \cdot 6\text{H}_2\text{O}$ (2.65 g), and HEPES (11.92 g) in millipore water (~400 mL). Adjust the mixture to pH = 7.5 with NaOH. Add water to make a total volume of 500 mL. Filter through a 0.2 μm filter (Nalgene). Store at 4 °C.

3.6.2.10 1 x ND96

Dilute 20 x ND96 (25 mL) with Millipore water (450 mL). To the mixture add Na-Pyruvate (138 mg) and theophyllen (60 mg). The solution was then adjusted to pH 7.5 with NaOH and then filtered through a 0.2 μm filter (Nalgene). Gentamicin (500 μL) was added. The osmolarity was checked to ensure that it is between 195 and 240.

3.7 References

1. Baulac, S.; Huberfeld, G.; Gourfinkel-An, I.; Mitropoulou, G.; Beranger, A.; Prud'homme, J. F.; Baulac, M.; Brice, A.; Bruzzone, R.; LeGuern, E., First genetic evidence of GABA(A) receptor dysfunction in epilepsy: a mutation in the gamma2-subunit gene. *Nat Genet* **2001**, 28, (1), 46-8.
2. Brune, W.; Weber, R. G.; Saul, B.; von Knebel Doeberitz, M.; Grond-Ginsbach, C.; Kellerman, K.; Meinck, H. M.; Becker, C. M., A GLRA1 null mutation in recessive hyperekplexia challenges the functional role of glycine receptors. *Am J Hum Genet* **1996**, 58, (5), 989-97.
3. Buckwalter, M. S.; Cook, S. A.; Davisson, M. T.; White, W. F.; Camper, S. A., A frameshift mutation in the mouse alpha 1 glycine receptor gene (Glr1) results in progressive neurological symptoms and juvenile death. *Hum Mol Genet* **1994**, 3, (11), 2025-30.
4. De Fusco, M.; Becchetti, A.; Patrignani, A.; Annesi, G.; Gambardella, A.; Quattrone, A.; Ballabio, A.; Wanke, E.; Casari, G., The nicotinic receptor beta 2 subunit is mutant in nocturnal frontal lobe epilepsy. *Nat Genet* **2000**, 26, (3), 275-6.
5. Elmslie, F. V.; Hutchings, S. M.; Spencer, V.; Curtis, A.; Covanis, T.; Gardiner, R. M.; Rees, M., Analysis of GLRA1 in hereditary and sporadic hyperekplexia: a novel mutation in a family cosegregating for hyperekplexia and spastic paraparesis. *J Med Genet* **1996**, 33, (5), 435-6.
6. Gunther, U.; Benson, J.; Benke, D.; Fritschy, J. M.; Reyes, G.; Knoflach, F.; Crestani, F.; Aguzzi, A.; Arigoni, M.; Lang, Y.; et al., Benzodiazepine-insensitive mice generated by targeted disruption of the gamma 2 subunit gene of gamma-aminobutyric acid type A receptors. *Proc Natl Acad Sci U S A* **1995**, 92, (17), 7749-53.
7. Hirose, S.; Iwata, H.; Akiyoshi, H.; Kobayashi, K.; Ito, M.; Wada, K.; Kaneko, S.; Mitsudome, A., A novel mutation of CHRNA4 responsible for autosomal dominant nocturnal frontal lobe epilepsy. *Neurology* **1999**, 53, (8), 1749-53.
8. Phillips, H. A.; Favre, I.; Kirkpatrick, M.; Zuberi, S. M.; Goudie, D.; Heron, S. E.; Scheffer, I. E.; Sutherland, G. R.; Berkovic, S. F.; Bertrand, D.; Mulley, J. C., CHRN2 is the second acetylcholine receptor subunit associated with autosomal dominant nocturnal frontal lobe epilepsy. *Am J Hum Genet* **2001**, 68, (1), 225-31.
9. Saenz, A.; Galan, J.; Caloustian, C.; Lorenzo, F.; Marquez, C.; Rodriguez, N.; Jimenez, M. D.; Poza, J. J.; Cobo, A. M.; Grid, D.; Prud'homme, J. F.; Lopez de Munain, A., Autosomal dominant nocturnal frontal lobe epilepsy in a Spanish family with a Ser252Phe mutation in the CHRNA4 gene. *Arch Neurol* **1999**, 56, (8), 1004-9.
10. Scheffer, I. E.; Bhatia, K. P.; Lopes-Cendes, I.; Fish, D. R.; Marsden, C. D.; Andermann, F.; Andermann, E.; Desbiens, R.; Cendes, F.; Manson, J. I.; et al., Autosomal dominant frontal epilepsy misdiagnosed as sleep disorder. *Lancet* **1994**, 343, (8896), 515-7.
11. Shiang, R.; Ryan, S. G.; Zhu, Y. Z.; Fielder, T. J.; Allen, R. J.; Fryer, A.; Yamashita, S.; O'Connell, P.; Wasmuth, J. J., Mutational analysis of familial and sporadic hyperekplexia. *Ann Neurol* **1995**, 38, (1), 85-91.
12. Shiang, R.; Ryan, S. G.; Zhu, Y. Z.; Hahn, A. F.; O'Connell, P.; Wasmuth, J. J., Mutations in the alpha 1 subunit of the inhibitory glycine receptor cause the dominant neurologic disorder, hyperekplexia. *Nat Genet* **1993**, 5, (4), 351-8.
13. Steinlein, O. K.; Magnusson, A.; Stoodt, J.; Bertrand, S.; Weiland, S.; Berkovic, S. F.; Nakken, K. O.; Propping, P.; Bertrand, D., An insertion mutation of the CHRNA4 gene in

a family with autosomal dominant nocturnal frontal lobe epilepsy. *Hum Mol Genet* **1997**, 6, (6), 943-7.

14. Steinlein, O. K.; Mulley, J. C.; Propping, P.; Wallace, R. H.; Phillips, H. A.; Sutherland, G. R.; Scheffer, I. E.; Berkovic, S. F., A missense mutation in the neuronal nicotinic acetylcholine receptor alpha 4 subunit is associated with autosomal dominant nocturnal frontal lobe epilepsy. *Nat Genet* **1995**, 11, (2), 201-3.

15. Kullmann, D. M., The neuronal channelopathies. *Brain* **2002**, 125, (Pt 6), 1177-95.

16. Ashcroft, F. M., *Ion channels and disease : channelopathies*. Academic Press: San Diego, 2000; p xxi, 481 p.

17. Yang, J., Ion permeation through 5-hydroxytryptamine-gated channels in neuroblastoma N18 cells. *J Gen Physiol* **1990**, 96, (6), 1177-98.

18. Yakel, J. L.; Shao, X. M.; Jackson, M. B., The selectivity of the channel coupled to the 5-HT₃ receptor. *Brain Res* **1990**, 533, (1), 46-52.

19. Huang, L. Y.; Catterall, W. A.; Ehrenstein, G., Selectivity of cations and nonelectrolytes for acetylcholine-activated channels in cultured muscle cells. *J Gen Physiol* **1978**, 71, (4), 397-410.

20. Dwyer, T. M.; Adams, D. J.; Hille, B., The permeability of the endplate channel to organic cations in frog muscle. *J Gen Physiol* **1980**, 75, (5), 469-92.

21. Cohen, B. N.; Labarca, C.; Davidson, N.; Lester, H. A., Mutations in M2 alter the selectivity of the mouse nicotinic acetylcholine receptor for organic and alkali metal cations. *J Gen Physiol* **1992**, 100, (3), 373-400.

22. Bertrand, D.; Galzi, J. L.; Devillers-Thiery, A.; Bertrand, S.; Changeux, J. P., Mutations at two distinct sites within the channel domain M2 alter calcium permeability of neuronal alpha 7 nicotinic receptor. *Proc Natl Acad Sci U S A* **1993**, 90, (15), 6971-5.

23. Bormann, J.; Hamill, O. P.; Sakmann, B., Mechanism of anion permeation through channels gated by glycine and gamma-aminobutyric acid in mouse cultured spinal neurones. *J Physiol* **1987**, 385, 243-86.

24. Fatima-Shad, K.; Barry, P. H., Anion permeation in GABA- and glycine-gated channels of mammalian cultured hippocampal neurons. *Proc Biol Sci* **1993**, 253, (1336), 69-75.

25. Samochocki, M.; Hoffle, A.; Fehrenbacher, A.; Jostock, R.; Ludwig, J.; Christner, C.; Radina, M.; Zerlin, M.; Ullmer, C.; Pereira, E. F.; Lubbert, H.; Albuquerque, E. X.; Maelicke, A., Galantamine is an allosterically potentiating ligand of neuronal nicotinic but not of muscarinic acetylcholine receptors. *J Pharmacol Exp Ther* **2003**, 305, (3), 1024-36.

26. Tanner, C. M.; Goldman, S. M.; Aston, D. A.; Ottman, R.; Ellenberg, J.; Mayeux, R.; Langston, J. W., Smoking and Parkinson's disease in twins. *Neurology* **2002**, 58, (4), 581-8.

27. Levin, E. D.; Connors, C. K.; Silva, D.; Hinton, S. C.; Meck, W. H.; March, J.; Rose, J. E., Transdermal nicotine effects on attention. *Psychopharmacology (Berl)* **1998**, 140, (2), 135-41.

28. Shytle, R. D.; Silver, A. A.; Wilkinson, B. J.; Sanberg, P. R., A pilot controlled trial of transdermal nicotine in the treatment of attention deficit hyperactivity disorder. *World J Biol Psychiatry* **2002**, 3, (3), 150-5.

29. Bruss, M.; Eucker, T.; Gothert, M.; Bonisch, H., Exon-intron organization of the human 5-HT_{3A} receptor gene. *Neuropharmacology* **2000**, 39, (2), 308-15.

30. Greenshaw, A. J., Behavioural pharmacology of 5-HT₃ receptor antagonists: a critical update on therapeutic potential. *Trends Pharmacol Sci* **1993**, 14, (7), 265-70.

31. Gyermek, L., 5-HT₃ receptors: pharmacologic and therapeutic aspects. *J Clin Pharmacol* **1995**, 35, (9), 845-55.
32. Barann, M.; Gothert, M.; Fink, K.; Bonisch, H., Inhibition by anaesthetics of ¹⁴C-guanidinium flux through the voltage-gated sodium channel and the cation channel of the 5-HT₃ receptor of N1E-115 neuroblastoma cells. *Naunyn Schmiedebergs Arch Pharmacol* **1993**, 347, (2), 125-32.
33. Downie, D. L.; Hope, A. G.; Belelli, D.; Lambert, J. J.; Peters, J. A.; Bentley, K. R.; Steward, L. J.; Chen, C. Y.; Barnes, N. M., The interaction of trichloroethanol with murine recombinant 5-HT₃ receptors. *Br J Pharmacol* **1995**, 114, (8), 1641-51.
34. Emerit, M. B.; Riad, M.; Fattaccini, C. M.; Hamon, M., Characteristics of [¹⁴C]guanidinium accumulation in NG 108-15 cells exposed to serotonin 5-HT₃ receptor ligands and substance P. *J Neurochem* **1993**, 60, (6), 2059-67.
35. Machu, T. K.; Harris, R. A., Alcohols and anesthetics enhance the function of 5-hydroxytryptamine₃ receptors expressed in *Xenopus laevis* oocytes. *J Pharmacol Exp Ther* **1994**, 271, (2), 898-905.
36. Peters, J. A.; Malone, H. M.; Lambert, J. J., Ketamine potentiates 5-HT₃ receptor-mediated currents in rabbit nodose ganglion neurones. *Br J Pharmacol* **1991**, 103, (3), 1623-5.
37. White, P. F.; Way, W. L.; Trevor, A. J., Ketamine--its pharmacology and therapeutic uses. *Anesthesiology* **1982**, 56, (2), 119-36.
38. Karlin, A., Structure of nicotinic acetylcholine receptors. *Curr Opin Neurobiol* **1993**, 3, (3), 299-309.
39. Corringer, P. J.; Le Novere, N.; Changeux, J. P., Nicotinic receptors at the amino acid level. *Annu Rev Pharmacol Toxicol* **2000**, 40, 431-58.
40. Mishina, M.; Takai, T.; Imoto, K.; Noda, M.; Takahashi, T.; Numa, S.; Methfessel, C.; Sakmann, B., Molecular distinction between fetal and adult forms of muscle acetylcholine receptor. *Nature* **1986**, 321, (6068), 406-11.
41. Sakmann, B.; Methfessel, C.; Mishina, M.; Takahashi, T.; Takai, T.; Kurasaki, M.; Fukuda, K.; Numa, S., Role of acetylcholine receptor subunits in gating of the channel. *Nature* **1985**, 318, (6046), 538-43.
42. Anand, R.; Conroy, W. G.; Schoepfer, R.; Whiting, P.; Lindstrom, J., Neuronal nicotinic acetylcholine receptors expressed in *Xenopus* oocytes have a pentameric quaternary structure. *J Biol Chem* **1991**, 266, (17), 11192-8.
43. Lindstrom, J.; Schoepfer, R.; Conroy, W.; Whiting, P.; Das, M.; Saedi, M.; Anand, R., The nicotinic acetylcholine receptor gene family: structure of nicotinic receptors from muscle and neurons and neuronal alpha-bungarotoxin-binding proteins. *Adv Exp Med Biol* **1991**, 287, 255-78.
44. Claudio, T.; Ballivet, M.; Patrick, J.; Heinemann, S., Nucleotide and deduced amino acid sequences of *Torpedo californica* acetylcholine receptor gamma subunit. *Proc Natl Acad Sci U S A* **1983**, 80, (4), 1111-5.
45. Noda, M.; Furutani, Y.; Takahashi, H.; Toyosato, M.; Tanabe, T.; Shimizu, S.; Kikuyotani, S.; Kayano, T.; Hirose, T.; Inayama, S.; et al., Cloning and sequence analysis of calf cDNA and human genomic DNA encoding alpha-subunit precursor of muscle acetylcholine receptor. *Nature* **1983**, 305, (5937), 818-23.
46. Smith, G. B.; Olsen, R. W., Functional domains of GABA_A receptors. *Trends Pharmacol Sci* **1995**, 16, (5), 162-8.

47. Karlin, A., Emerging structure of the nicotinic acetylcholine receptors. *Nat Rev Neurosci* **2002**, 3, (2), 102-14.
48. Conti-Tronconi, B. M.; Raftery, M. A., The nicotinic cholinergic receptor: correlation of molecular structure with functional properties. *Annu Rev Biochem* **1982**, 51, 491-530.
49. Changeux, J. P.; Devillers-Thiery, A.; Chemouilli, P., Acetylcholine receptor: an allosteric protein. *Science* **1984**, 225, (4668), 1335-45.
50. Unwin, N., Acetylcholine receptor channel imaged in the open state. *Nature* **1995**, 373, (6509), 37-43.
51. Unwin, N., Structure and action of the nicotinic acetylcholine receptor explored by electron microscopy. *FEBS Lett* **2003**, 555, (1), 91-5.
52. Miyazawa, A.; Fujiyoshi, Y.; Unwin, N., Structure and gating mechanism of the acetylcholine receptor pore. *Nature* **2003**, 423, (6943), 949-55.
53. Sigel, E.; Buhr, A.; Baur, R., Role of the conserved lysine residue in the middle of the predicted extracellular loop between M2 and M3 in the GABA(A) receptor. *J Neurochem* **1999**, 73, (4), 1758-64.
54. Shan, Q.; Nevin, S. T.; Haddrill, J. L.; Lynch, J. W., Asymmetric contribution of alpha and beta subunits to the activation of alphabeta heteromeric glycine receptors. *J Neurochem* **2003**, 86, (2), 498-507.
55. Rovira, J. C.; Vicente-Agullo, F.; Campos-Caro, A.; Criado, M.; Sala, F.; Sala, S.; Ballesta, J. J., Gating of alpha3beta4 neuronal nicotinic receptor can be controlled by the loop M2-M3 of both alpha3 and beta4 subunits. *Pflugers Arch* **1999**, 439, (1-2), 86-92.
56. Rovira, J. C.; Ballesta, J. J.; Vicente-Agullo, F.; Campos-Caro, A.; Criado, M.; Sala, F.; Sala, S., A residue in the middle of the M2-M3 loop of the beta4 subunit specifically affects gating of neuronal nicotinic receptors. *FEBS Lett* **1998**, 433, (1-2), 89-92.
57. O'Shea, S. M.; Harrison, N. L., Arg-274 and Leu-277 of the gamma-aminobutyric acid type A receptor alpha 2 subunit define agonist efficacy and potency. *J Biol Chem* **2000**, 275, (30), 22764-8.
58. Lynch, J. W.; Rajendra, S.; Pierce, K. D.; Handford, C. A.; Barry, P. H.; Schofield, P. R., Identification of intracellular and extracellular domains mediating signal transduction in the inhibitory glycine receptor chloride channel. *Embo J* **1997**, 16, (1), 110-20.
59. Lewis, T. M.; Sivilotti, L. G.; Colquhoun, D.; Gardiner, R. M.; Schoepfer, R.; Rees, M., Properties of human glycine receptors containing the hyperekplexia mutation alpha1(K276E), expressed in *Xenopus* oocytes. *J Physiol* **1998**, 507 (Pt 1), 25-40.
60. Kusama, T.; Wang, J. B.; Spivak, C. E.; Uhl, G. R., Mutagenesis of the GABA rho 1 receptor alters agonist affinity and channel gating. *Neuroreport* **1994**, 5, (10), 1209-12.
61. Deane, C. M.; Lummis, S. C., The role and predicted propensity of conserved proline residues in the 5-HT3 receptor. *J Biol Chem* **2001**, 276, (41), 37962-6.
62. Davies, M.; Newell, J. G.; Dunn, S. M., Mutagenesis of the GABA(A) receptor alpha1 subunit reveals a domain that affects sensitivity to GABA and benzodiazepine-site ligands. *J Neurochem* **2001**, 79, (1), 55-62.
63. Campos-Caro, A.; Sala, S.; Ballesta, J. J.; Vicente-Agullo, F.; Criado, M.; Sala, F., A single residue in the M2-M3 loop is a major determinant of coupling between binding and gating in neuronal nicotinic receptors. *Proc Natl Acad Sci U S A* **1996**, 93, (12), 6118-23.
64. Bera, A. K.; Chatav, M.; Akabas, M. H., GABA(A) receptor M2-M3 loop secondary structure and changes in accessibility during channel gating. *J Biol Chem* **2002**, 277, (45), 43002-10.

65. Kash, T. L.; Jenkins, A.; Kelley, J. C.; Trudell, J. R.; Harrison, N. L., Coupling of agonist binding to channel gating in the GABA(A) receptor. *Nature* **2003**, 421, (6920), 272-5.
66. Lynch, J. W.; Han, N. L.; Haddrill, J.; Pierce, K. D.; Schofield, P. R., The surface accessibility of the glycine receptor M2-M3 loop is increased in the channel open state. *J Neurosci* **2001**, 21, (8), 2589-99.
67. Grosman, C.; Salamone, F. N.; Sine, S. M.; Auerbach, A., The extracellular linker of muscle acetylcholine receptor channels is a gating control element. *Journal of General Physiology* **2000**, 116, (3), 327-339.
68. Castillo, M.; Mulet, J.; Bernal, J. A.; Criado, M.; Sala, F.; Sala, S., Improved gating of a chimeric alpha7-5HT3A receptor upon mutations at the M2-M3 extracellular loop. *FEBS Lett* **2006**, 580, (1), 256-60.
69. Schimmel, P. R.; Flory, P. J., Conformational energies and configurational statistics of copolypeptides containing L-proline. *J Mol Biol* **1968**, 34, (1), 105-20.
70. MacArthur, M. W.; Thornton, J. M., Influence of proline residues on protein conformation. *J Mol Biol* **1991**, 218, (2), 397-412.
71. Chakrabarti, P.; Pal, D., The interrelationships of side-chain and main-chain conformations in proteins. *Prog Biophys Mol Biol* **2001**, 76, (1-2), 1-102.
72. Bhattacharyya, R.; Chakrabarti, P., Stereospecific interactions of proline residues in protein structures and complexes. *J Mol Biol* **2003**, 331, (4), 925-40.
73. Stewart, D. E.; Sarkar, A.; Wampler, J. E., Occurrence and role of cis peptide bonds in protein structures. *J Mol Biol* **1990**, 214, (1), 253-60.
74. Weiss, M. S.; Jabs, A.; Hilgenfeld, R., Peptide bonds revisited. *Nat Struct Biol* **1998**, 5, (8), 676.
75. Song, J.; Burrage, K.; Yuan, Z.; Huber, T., Prediction of cis/trans isomerization in proteins using PSI-BLAST profiles and secondary structure information. *BMC Bioinformatics* **2006**, 7, 124.
76. Pal, D.; Chakrabarti, P., Cis peptide bonds in proteins: residues involved, their conformations, interactions and locations. *J Mol Biol* **1999**, 294, (1), 271-88.
77. Jabs, A.; Weiss, M. S.; Hilgenfeld, R., Non-proline cis peptide bonds in proteins. *J Mol Biol* **1999**, 286, (1), 291-304.
78. Vanhoof, G.; Goossens, F.; De Meester, I.; Hendriks, D.; Scharpe, S., Proline motifs in peptides and their biological processing. *Faseb J* **1995**, 9, (9), 736-44.
79. Huang, G. C.; Zhou, J. M., The two slow refolding processes of creatine kinase are catalyzed by cyclophilin. *J Protein Chem* **2000**, 19, (4), 285-9.
80. Kamen, D. E.; Woody, R. W., Identification of proline residues responsible for the slow folding kinetics in pectate lyase C by mutagenesis. *Biochemistry* **2002**, 41, (14), 4724-32.
81. Kamen, D. E.; Woody, R. W., Folding kinetics of the protein pectate lyase C reveal fast-forming intermediates and slow proline isomerization. *Biochemistry* **2002**, 41, (14), 4713-23.
82. Kim, D. H.; Jang, D. S.; Nam, G. H.; Choi, K. Y., Folding mechanism of ketosteroid isomerase from *Comamonas testosteroni*. *Biochemistry* **2001**, 40, (16), 5011-7.
83. Slupsky, C. M.; Sykes, D. B.; Gay, G. L.; Sykes, B. D., The HoxB1 hexapeptide is a prefolded domain: implications for the Pbx1/Hox interaction. *Protein Sci* **2001**, 10, (6), 1244-53.

84. Stukenberg, P. T.; Kirschner, M. W., Pin1 acts catalytically to promote a conformational change in Cdc25. *Mol Cell* **2001**, 7, (5), 1071-83.
85. von Ahsen, O.; Lim, J. H.; Caspers, P.; Martin, F.; Schonfeld, H. J.; Rassow, J.; Pfanner, N., Cyclophilin-promoted folding of mouse dihydrofolate reductase does not include the slow conversion of the late-folding intermediate to the active enzyme. *J Mol Biol* **2000**, 297, (3), 809-18.
86. Reimer, U.; Fischer, G., Local structural changes caused by peptidyl-prolyl cis/trans isomerization in the native state of proteins. *Biophys Chem* **2002**, 96, (2-3), 203-12.
87. Keller, M.; Boissard, C.; Patiny, L.; Chung, N. N.; Lemieux, C.; Mutter, M.; Schiller, P. W., Pseudoproline-containing analogues of morphiceptin and endomorphin-2: evidence for a cis Tyr-Pro amide bond in the bioactive conformation. *J Med Chem* **2001**, 44, (23), 3896-903.
88. Mierke, D. F.; Nossner, G.; Schiller, P. W.; Goodman, M., Morphiceptin analogs containing 2-aminocyclopentane carboxylic acid as a peptidomimetic for proline. *Int J Pept Protein Res* **1990**, 35, (1), 35-45.
89. Yamazaki, T.; Probsti, A.; Schiller, P. W.; Goodman, M., Biological and conformational studies of [Val4]morphiceptin and [D-Val4]morphiceptin analogs incorporating cis-2-aminocyclopentane carboxylic acid as a peptidomimetic for proline. *Int J Pept Protein Res* **1991**, 37, (5), 364-81.
90. Nielsen, K. J.; Watson, M.; Adams, D. J.; Hammarstrom, A. K.; Gage, P. W.; Hill, J. M.; Craik, D. J.; Thomas, L.; Adams, D.; Alewood, P. F.; Lewis, R. J., Solution structure of mu-conotoxin PIIIA, a preferential inhibitor of persistent tetrodotoxin-sensitive sodium channels. *J Biol Chem* **2002**, 277, (30), 27247-55.
91. Feng, Y.; Hood, W. F.; Forgey, R. W.; Abegg, A. L.; Caparon, M. H.; Thiele, B. R.; Leimgruber, R. M.; McWherter, C. A., Multiple conformations of a human interleukin-3 variant. *Protein Sci* **1997**, 6, (8), 1777-82.
92. Halab, L.; Lubell, W. D., Use of Steric Interactions To Control Peptide Turn Geometry. Synthesis of Type VI beta-Turn Mimics with 5-tert-Butylproline. *J Org Chem* **1999**, 64, (9), 3312-3321.
93. Belec, L.; Slaninova, J.; Lubell, W. D., A study of the relationship between biological activity and prolyl amide isomer geometry in oxytocin using 5-tert-butylproline to augment the Cys(6)-Pro(7) amide cis-isomer population. *J Med Chem* **2000**, 43, (8), 1448-55.
94. Mallis, R. J.; Brazin, K. N.; Fulton, D. B.; Andreotti, A. H., Structural characterization of a proline-driven conformational switch within the Itk SH2 domain. *Nat Struct Biol* **2002**, 9, (12), 900-5.
95. Beausoleil, E.; LArcheveque, B.; Belec, L.; Atfani, M.; Lubell, W. D., 5-tert-butylproline. *Journal of Organic Chemistry* **1996**, 61, (26), 9447-9454.
96. Koskinen, A. M. P.; Rapoport, H., Synthesis of 4-Substituted Prolines as Conformationally Constrained Amino-Acid Analogs. *Journal of Organic Chemistry* **1989**, 54, (8), 1859-1866.